SYNTHESIS OF MAGNETIC FERRITE COATED ON MESOPOROUS SILICA NANOSTRUCTURES

By

Sidra Anis Farooqi

(248-FBAS/MSPHY/S14)

DEPARTMENT OF PHYSICS

FACULTY OF BASIC AND APPLIED SCIENCES

INTERNATIONAL ISLAMIC UNIVERSITY

ISLAMABAD

(2016)

Magnetism

Nanotechnology

Cobalt ferrite

SYNTHESIS OF MAGNETIC FERRITE COATED ON MESOPOROUS SILICA NANOSTRUCTURE

By

Sidra Anis Farooqi

(248-FBAS/MSPHY/S14)

Supervisor

Dr Shamaila Sajjad

DEPARTMENT OF PHYSICS

FACULTY OF BASIC AND APPLIED SCIENCES

INTERNATIONAL ISLAMIC UNIVERSITY

ISLAMABAD

(2016)

INTERNATIONAL ISLAMIC UNIVERSITY, ISLAMABAD

FACULTY OF BASIC AND APPLIED SCIENCES

DEPARTMENT OF PHYSICS

SYNTHESIS OF MAGNETIC FERRITE COATED ON MESOPOROUS SILICA NANOSTRUCTURE

By

Sidra Anis Farooqi

(Registration No. 248-FBAS/MSPHY/S14)

A thesis submitted to

Department of Physics

For the award of the degree of

MS Physics

Signature: _____

Dr. Shagufta Sajjad
Chairperson
Department of Physics (FC, FBAS)
International Islamic University
Islamabad

(Chairman, Department of Physics)

Signature: _____

(Dean FBAS, IIU, Islamabad)

INTERNATIONAL ISLAMIC UNIVERSITY, ISLAMABAD
FACULTY OF BASIC AND APPLIED SCIENCES
DEPARTMENT OF PHYSICS

Dated: 29-01-2016

FINAL APPROVAL

It is certified that the work presented in this thesis entitled "**SYNTHESIS OF MAGNETIC FERRITE COATED ON MESOPOROUS SILICA NAOSTRUCTURES**" by **Ms. Sidra Anis Farooqi** bearing **Registration No. 248-FBAS/MSPHY/S14** is of sufficient standard in scope and quality for the award of degree of MS Physics from International Islamic University, Islamabad.

COMMITTEE

External Examiner

Dr. Tariq Mehmood

Associate Professor,

National Centre of Physics

Internal Examiner

Dr Waqar Adil

Associate Professor,

Department of Physics, FBAS, IIUI

Supervisor

Dr Shamiala Sajjad

Assistant Professor,

Department of Physics, FBAS, IIUI

Co-Supervisor

Dr. Sajjad Ahmed Khan Leghari

Principal Scientist,

PAEC, Islamabad

A thesis submitted to

Department of Physics

International Islamic University Islamabad

as a partial fulfillment for the award of the degree of

MS in Physics

Declaration

I hereby declare that this thesis work, neither as a whole nor a part of it has been copied out from any source. Further, work presented in this dissertation has not been submitted in support of any application for any other degree or qualification to any other university or institute and is considerable under the plagiarism rules of Higher Education Commission (HEC), Pakistan.

Sidra Anis Farooqi

(248-FBAS/MSPHY/S14)

DEDICATION

T0

My loving Parents

Who never stop giving of themselves in myriad ways. Words become worthless when I look at them as an icon of endless forte, inspiration, and encouragement for being what I am today. May Allah please grant them infinite pleasure, peace of soul and protect them from all danger.

Acknowledgements

In the name of Allah (SWT), the most Merciful, the most beneficent. Praise is only for Allah, the Master of the Day of Judgement and the Lord of Universe. I am grateful to Allah who created us, to whom we have to submit and return, who gave us knowledge and wisdom. I would like to express my sincere gratitude to my advisor **Dr. Shamaila Sajjad** for the continuous support of my MS study and research, for her patience, motivation, enthusiasm and immense knowledge. Her guidance helped me in all the time of research and writing of this thesis. Besides my advisor, I would like to thank **Dr. Sajjad Ahmad Khan** and rest of my thesis committee members.

I would like to thank Government College University, Lahore for X-Ray Diffraction analysis (XRD) and Institute of Space technology, Islamabad for Scanning Electron Microscopy and National Center for Physics for UV-Visible spectroscopy. I would like to thanks,Department of Physics International Islamic University, Islamabad for Fourier transform infra-red spectroscopy (FTIR). I would like special thanks to Department of Chemistry, Allama Iqbal Open University, Islamabad for providing me the chance to work in the great environment of laboratories which were best for research purpose.

I have no words to acknowledge the sacrifices, efforts, lots of prayers, guidance, support, encouragement and firm dedication of my mother and my father.

Last but not least, I am very obliged to my well-wishers and my friends **Ryma, Sania** and all my classmates for their continuous support and encouragement that has led me to pursue this degree.

Sidra Anis Farooqi

Contents

Preface

This work presented in this thesis has been carried out at laboratory, Department of Physics, Faculty of Basic and Applied Sciences, International Islamic University, Islamabad. The thesis is divided in to four chapters. First chapter gives brief introduction. Chapter two discusses fabrication and preparation of the sample. Chapter three Consists of characterization techniques for investigation of samples. Chapter four describes the effect of coating on structural, chemical and magnetic properties of mesoporous silica nanoparticles. At the end, there is an overall conclusion of the thesis. References to the literature are mentioned at the end.

Abstract

The nanoparticles of mesoporous silica have been synthesized using Hydrothermal and Greener route. In order to enhance the physical properties, the prepared samples of silica have been annealed at 550°C. We coated silica with cobalt ferrite nanoparticles, which were synthesized by greener route. Characterization of synthesized particles was done by using characterize tools. The structural investigation was done by X-Ray Diffraction (XRD).The morphology of the samples has been checked using scanning electron microscopy (SEM). The composition of cobalt ferrite and silica have been determined by using electron dispersive X-Ray spectroscopy (EDX).Fourier transform infra-red spectroscopy (FTIR) confirmed the characteristic energy bands.By using UV-visible spectroscopy band gap is calculated. The coating of cobalt ferrite on mesoporous silica nanoparticles have shown enhancement in magnetic moment. The observed characteristics of cobalt ferrite coated mesoporous silica nanoparticles are the rising candidate for Nanomedicine and Dug Delivery Applications.

Index of Figure

Index of table

List of Abbreviations

NPs	Nanoparticles
nm	nanometer
SBA	Santa Barbara Amorphous
MSNs	Mesoporous silica Nanoparticles
HMS	hexagonal mesoporous silica
MFA	Magnetic fluid Hypertermia
MRI	Magnetic Resonance Imaging
DNA	Deoxyribonucleic Acid
TEOS	Tetraethylorthosilicate
CTAB	Cetyltrimethylammonium Bromide
PBS	Phosphate-buffered saline
XRD	X-Ray Diffraction
SEM	Scanning Electron Microscopy
CL	Cathodoluminescene
SE	Secondary Electron
EDX	Energy Dispersive X-Ray spectroscopy
FTIR	Fourier transform infra-red spectroscopy
VSM	Vibrating Sample Magnetometer

List of Symbols

π	Pi
σ	Sigma
θ	Angle
λ	Wavelength
μ	Magnetic Dipole Moment

Chapter No. 1

Introduction

1.1 Nanotechnology or Nanoscience:

Over the past decade, a small word Nano is rapidly getting famous into world consciousness because of its great potential. The meaning of the prefix Nano is one billionth of a meter. The scale with range 1 to 100 nm is said to be a nanoscale. Nanoscience is the study and understanding of basic principles of molecules and structures having at least one of their dimensions in the nanometer (1 nm = 10^{-10}) range. These materials are known as Nanostructures while Nanotechnology is the synthesis, characterization and applications of these nanomaterials into useful Nano-devices.

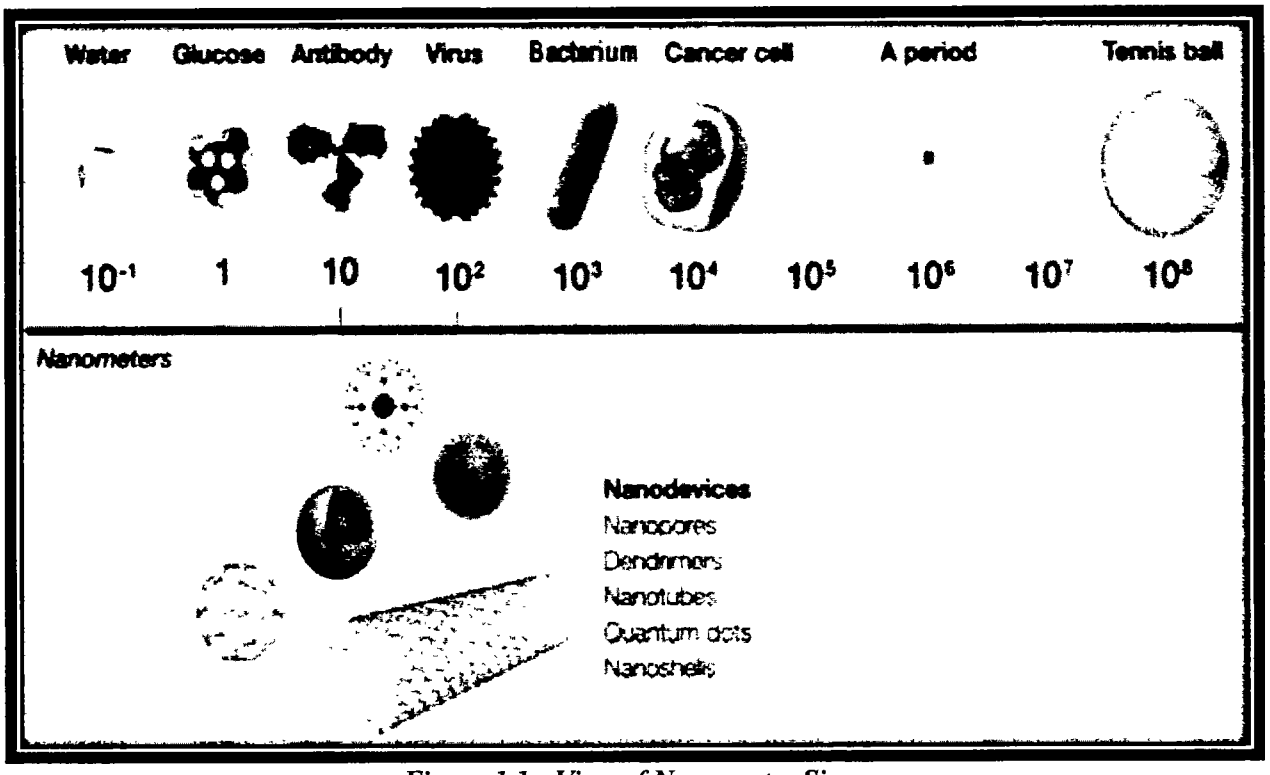

Figure 1.1: View of Nano meter Size

Nanostructures are the smallest possible solid things we have made up to date. Thus, nanostructures are in between single atom and bulk substantial. Quantum mechanics refer to

absolute compactness. Thus, quantum effects are required to understand properties of Nano-objects. For example, the smallest cluster of atoms called Quantum dots, Nanodots, and Nanoparticles. The chemical and physical properties of nanostructures are different as compared to the bulk material of the same composition because of high surface area to volume ratio of atoms at the nanoscale.

The properties of nanomaterials are size dependent so the suitable tuning of the properties of nanostructures by changing their size leads to useful applications in technology. The exterior atoms on the surface of particles have lower coordination number as compared to the interior atoms so increase in surface area to volume ratio by decreasing the size of nanostructure cause the behavior of surface of surface atoms to be dominant. Now a day Nanotechnologies are the emergent zone of scientists in all over the world. Nanoscale science is giving us with astonishing considerate and controller of matter at its ultimate dynamic side by side at the smaller scales. In real, nanoscale particles have apprehensive much contemplation due to their peculiar electronic [1], optical [2] and magnetic [3] possessions. The dimensions of these nanoparticles (NPs) mark them decisive contenders for the formation of competent nanostructures. Such alterations of NPs facilitate their use in biomedical Applications [4].

Medicine has countless future prospects built on the use of nanomaterials. In the last several decade, Nanomedicine has experienced quick progress [5-12]. The objective of Nanomedicine is to plan and manufacture drug delivery vehicles. These vehicles can transmit appropriate drug loads, proficiently cross-functional hurdles to influence target sites, and securely and sustainably antidote diseases. Many organic Nanomedicines, containing polymeric micelles, liposomes, dendrimers, drug polymer conjugates, and nanoparticles (NPs) have been widely considered as drug delivery schemes. Each delivery stage has its benefit and drawback.

1.2 Green Nanotechnology:

Nanomaterials make available resolutions to scientific and environmental tasks in the regions of solar energy conversion, medicine, catalysis and water treatment [13, 14]. This cumulative demand must be attended by "Green" synthesis methods. In the global struggles to reduce spawned harmful waste, "Green" chemistry and chemical processes are gradually participating with contemporary advances in science and industry. Green chemistry is defined as developing and implementing experimental designs of chemical procedure and products to minimize and banish hazardous

substances to human health and the environment. 12 principle of green chemistry is shown in figure 1.2. These principles are geared to guide in reducing the usage of insecure products and make the best use of the proficiency of natural procedures.

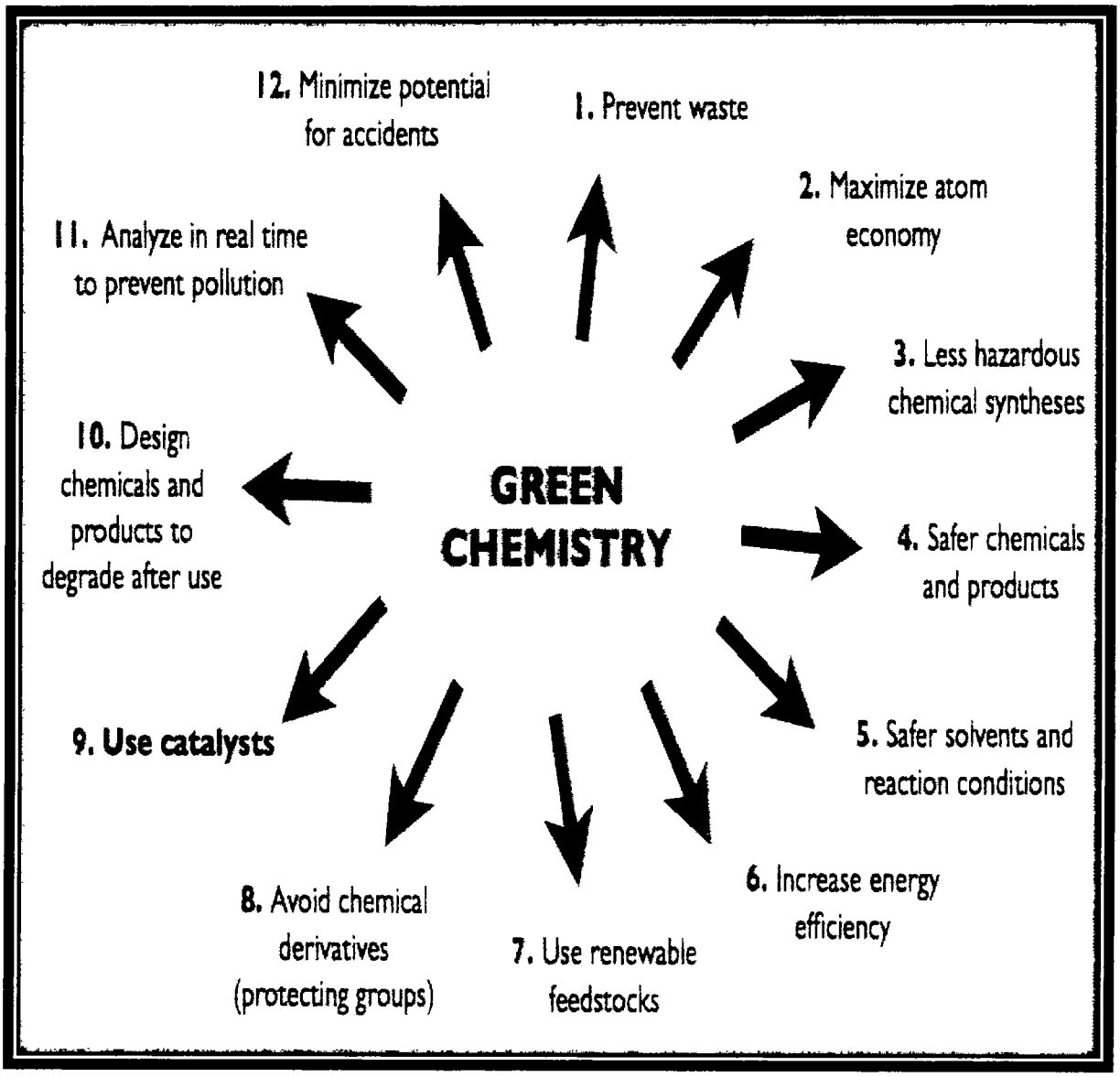

Figure 1.2: Fundamental principle of green chemistry

Therefore, any synthetic method or chemical process should discourse these principles by using environmentally caring solvents and safe chemicals [18]. Production of nanoparticles using biological means, especially plants is biocompatible as they conceal useful biomolecules which aggressively reduce metal ions [22, 23]. Additionally, plants as a biological means are biodegradable and so are the reducing and capping agents involved in the production process [24,

25]. In figure 1.3 there is a Schematic representation of plant as a source of green Nano synthesis and its uses in biomedical Application.

With the use of green chemistry, green nanotechnology, therefore, means making nanotechnology processes and products more environmentally friendly and energy efficient [15]. The goals of green nanotechnology are:

- Manufacturing Nano products using non-toxic ingredients, fewer energy sources at low temperature.
- Producing nanomaterials which are not harmful to both environment and human health.
- Producing Nano products that can provide a solution to environmental challenges [15, 17].

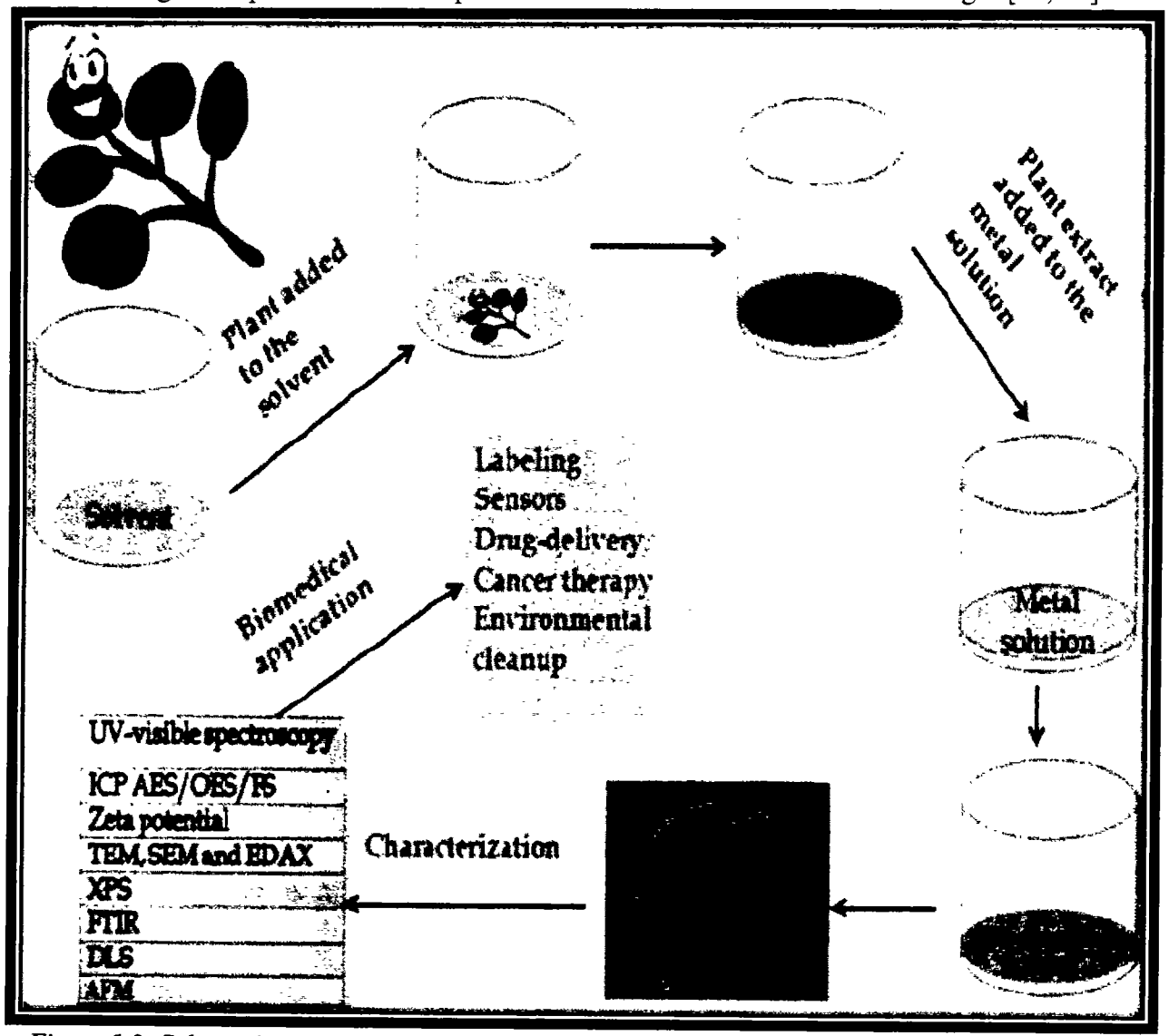

Figure 1.3: Schematic representation of plant as a source of green Nano synthesis, its characterization and biomedical Application [16]

1.3 Classification of Nanomaterials:

To understand the value and assortment of Nanomaterial it is essential to categorize them. The most divergent way of classification is on the basis of dimension [26]. Generally, we classified nanomaterials in four classes. As shown in figure 1.4.

i. 0 dimensional (0-D)

ii. 1 dimensional (1-D)

iii. 2 dimensional (2-D)

iv. 3 dimensional (3-D)

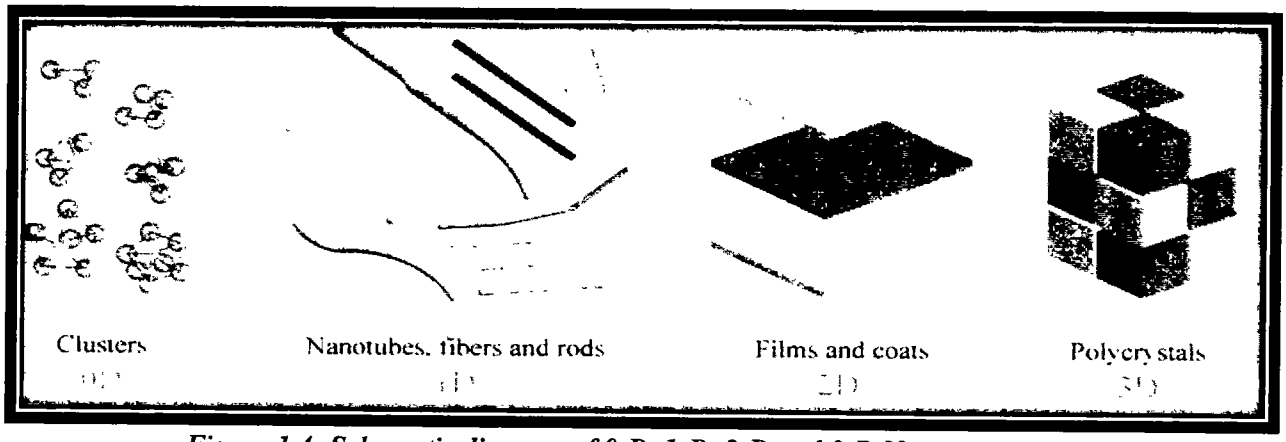

Figure 1.4: Schematic diagram of 0-D, 1-D, 2-D and 3-D Nano materials

1.3.1 Zero dimensional:

The material having all of its dimensions in nanometer scale denoted as zero-dimensional (0-D) materials. For example nanoparticles, nanoclusters etc. some of the physiognomies of (0-D) materials are given below:

- It may be amorphous or crystalline (single or poly)
- Can exist in different forms
- It can exist in single or matrix form
- It can be polymer or ceramic

1.3.2 One-dimensional:

The material having one of its dimension beyond Nanoscale. Those beyond give needle-like shape morphology. For example Nanowires, Nanotubes, Nanorods etc. some of the physiognomies of 1-D materials are given as:

- It may be amorphous or crystalline (single or poly)

- Chemically pure or impure

It can exist in single or matrix form

1.3.3 Two-dimensional:

Materials having two of its dimensions outside the Nanoscale. This will impart layers type structure to nanomaterials. For example Nanofilms and Nano coating etc. some of the possessions of 2-D materials are given below:

- Single layer or multi-layer structure
- Deposited on substrate
- Surrounded by matrix material
- Polymeric, metallic or ceramic

1.3.4 Three-dimensional:

The Materials having no dimension in nanoscale or having three dimensions exceeding Nanoscale are referred to as 3-dimensional materials. Three-dimensional materials are also called as bulk material. Although there is no atomic scale dimension but they have Nanoscale possessions. Some of the possessions of 3-D materials are given below:

- Composite material
- Multi-layered
- Chemically pure or impure

1.4 Mesoporous silica:

Mesoporous silica is amorphous inorganic materials which has silicon and oxygen atoms in their structure. Mesoporous shows that the pore dimensions in such materials range from 2-50 nm in dimension. Mesoporous Silica NPs have fascinated important attention because of their exceptional properties agreeable for in vivo applications [27-30]. Such as hydrophilic surface preferring prolonged circulation, multipurpose silane chemistry for surface functionalization, tremendous biocompatibility, a comfort of large-scale synthesis, and low price of NP fabrication. Mesoporous silica is also water soluble, chemically and thermally established with mechanical power and are toxicologically harmless. At the superficial of the mesoporous silica materials, there are silanol assemblies that can be applied for enzyme halt by hydrogen bonding between hydroxyl groups and carbonyl or amino groups on enzyme molecules.

Mesoporous silica materials can be synthesized in the presence of surfactants. The surfactant is crucial since it will decide the size of the formed pores and a wide variety of different surfactants can be used. Mostly surfactant used in mesoporous synthesis is non-ionic block copolymers. Benefits with block copolymers are their constancy to time is the assembling by fluctuating solvent composition, molecular weight or copolymer configuration. The size of the pores can also be controlled by using diverse temperatures for the duration of synthesis, where high temperature provides greater pores. The surfactant acts as templates for the polycondensation of the silicon source (sodium silicate, Tetraethylorthosilicate) [31, 32]. The features which conclude the physiochemical factors of mesoporous silica like a type of mesostructured, pore diameter, pore volume, wall thickness are hooked on the synthesis state of affairs such as pH of the medium, type of the silicon source, a templating agent and its attentiveness [33-35]. The nature of synthesis conditions will vary the superficial features of the mesoporous silica (silica-surfactant interactions). The nature of the superficial concluded silanol groups will diverge consequently in different mesoporous silica. The different types of silanol groups which are present on the surface of mesoporous silica are: (a) single, (b) hydrogen bonded, and (c) geminal silanol groups [36].

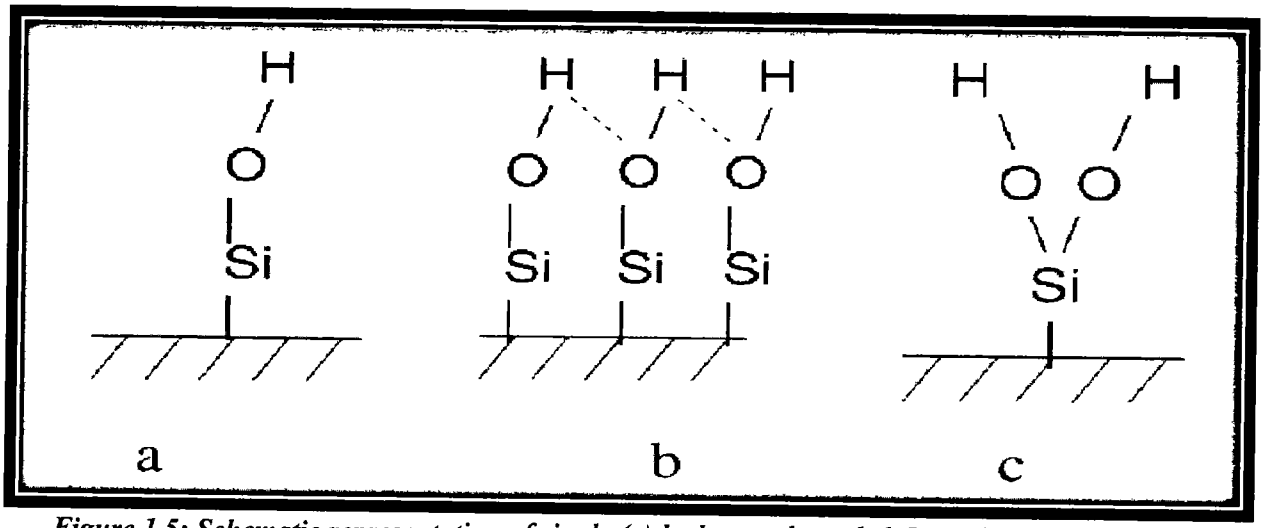

Figure 1.5: Schematic representation of single (a) hydrogen-bounded (b) and geminal (c) silanol groups present on the surface of mesoporous silica [36]

The content of the silanol groups is determined by how the silica-surfactant exchanges are cracked or on how surfactants are aloof, once silica materialization is complete. Due to the occurrence of these silanol groups at the surface of mesoporous silica, these materials are of specific concern because of tailorable superficial amendments [37, 38].

1.4.1 Applications:

Mesoporous silica materials have great surface areas, tunable pore diameters, great pore volumes and well-ordered absorbency which mark them possible contenders for various applications. The chemical nature and the capability to tailor the surface for chemical alteration as talk over above marks them supreme for applications such as adsorption, catalysis, separation, sensors and drug delivery systems [39-42]. Mesoporous silica has been used expansively in chromatographic columns for the parting of molecules and the halt of biomolecules such as enzymes [43, 44]. The combination of aluminum species in mesoporous silica provides them a fascinating character to catalyze reactions [45-52]. Mesoporous silica has also established their tactic in environmental and biomedical applications [53-58].

Nowadays, Green energy become a hot issue in both exploration and the world, whereas mesoporous silica has a significant place also here. SBA-15 uses as a template for the anode or cathode materials for batteries [59-61]. Additionally, it can also be used in solar cell applications, both as a template for an amalgamation of Titania or cobalt nanoparticles [12, 62-65] and as a scattering layer for refining the cell effectiveness [66]. Core-shell Nanocomposites of magnetite-mesoporous silica are widely used in environmentally friendly applications for the adsorption of noxious ions [67, 68].

1.4.1.1 Silica as a Nano medicine:

The traditional cure methods ultimately depend on cytotoxic medicines with terrifying side effects and deficient target specificity. To overcome this problem we should need to cultivate effective target specific drug delivery system [27, 69]. Following are the circumstance for the advancement of a proficient drug delivery system.

- Biocompatible carrier
- High loading drug
- Well-ordered release of drug at a proper rate
- No leakage of drug molecule; zero premature release
- Site directing and cell specificity ability

Biodegradable material like polymeric nanoparticle, dendrimers and liposomes were established as smart drug delivery system with target specificity triggering the carrier at particular pH or physiological conditions. But soft materials and the particle starts permeable. Silica has been well-

known as biocompatible among various fundamentally stable material. It has been shown that mesoporous structure of silica can stock and gradually release the drug e.g. MCM-41 and SBA-51 silicas. Mesoporous silica nanoparticle is honey-comb like porous structure with empty channels to encapsulate compounds. Following possessions of silica fascinated consideration for controlled drug delivery application:

- Tunable particle size: Mesoporous silica nanoparticle has tunable pre-size (10-300 nm) allowing endocytosis by living cells without causing remarkable cytotoxicity.
- Stable and Rigid Frame Work: As compared to others polymeric carrier Mesoporous silica nanoparticle are moderately stable and resistant to heat, pH, mechanical stress or other degradations.
- Uniform and Tunable Pore Size: Mesoporous silica nanoparticle has tunable pre-size (2-6 nm) with slender distribution. The property sanctions precision in drug delivery system.
- High Surface Area and Large Pore Volume: Mesoporous silica nanoparticle have a large surface area (N900m^2/g) and pore volume (N 0.9 cm^3/ g) allows high loading of the drug.
- Two Functional Surfaces: The two surfaces of Mesoporous silica nanoparticle i-e External (exterior) and internal (pore) sanctions external and internal functionalization of particles.
- Porous Structure: Mesoporous silica nanoparticle includes an exclusive honeycomb-like porous structure with cylindrical pore from one end to another end of a sphere. There is no connectivity between channels making it a good reservoir of the drug even in incomplete capping until capping is done [27, 70].

As mesoporous silica have high surface areas and pore volumes so it has great attention in the biomedical applications. They have been broadly researched as hopeful drug delivery systems. Mesoporous silica NPs are largely used for delivery of energetic payloads based on physical or chemical adsorption [27, 29].The literature precedent shows various illustrations of drug molecules loaded onto mesoporous silica materials. Ibuprofen has been broadly considered as a model drug adsorbed on the mesoporous silica materials like MCM-41, SBA-15 and hexagonal mesoporous silica (HMS) materials [71-74]. In addition, many anti-cancer drugs, such as doxorubicin and camptothecin, have also been studied for controlled release using mesoporous silica materials. Lin and co-workers studied the release of a drug cargo using crowned mesoporous silica materials. Recently, rattle type mesoporous silica Fe_3O_4@SiO_2 have also fascinated a great compact of attention for drug delivery [75, 76]. Drug delivery using mesoporous silica materials mostly be

contingent on the textural properties of these materials, such as pore diameters, pore volumes, particle morphology and surface amendments. The capability to cartel these possessions makes silica nanoparticles a wanted platform for biomedical imaging, analyzing, monitoring, and ablative rehabilitations [28].

1.5 Magnetic nanoparticles:

Nano-sized magnetic materials are of particular interest because the magnetic properties change drastically when the size of a magnetic particle is reduced below 100 nm and the modified attributes are useful for many applications and devices [77-79].

In large particles, energetic considerations favor the establishment of magnetic fields. As the particle size decreases toward some critical size, formation of domain walls becomes energetically unfavorable and the particles are called single domain. A number of interesting magnetic phenomena arise when one or more of the dimensions of a magnetic particle are reduced to nanometer size, that are of the order of single domains. Ferro- and Ferrimagnetic nanoparticles reveal an actions related to paramagnetism and it is half-way between Ferro/Ferrimagnetism and paramagnetism. These particles are called superparamagnetic particles.

Nanomagnetism emerged as a major field of research in the recent years due to the possible applications of the Nano-sized magnetic materials. Magnetic NPs have many distinctive magnetic possessions such as superparamagnetic, great coercively, small Curie temperature, high magnetic vulnerability, etc. Magnetic NPs are of big interest for researchers from a spacious range of fields, containing magnetic fluids, data storage, catalysis, and bio applications [74-78].

Currently, magnetic NPs are also employed in important bioapplications, including magnetic bioseparation and detection of biological entities (cell, protein, nucleic acids, enzyme, bacteria virus, etc.), clinic diagnosis and therapy (such as MRI (magnetic resonance image) and MFH (magnetic fluid hyperthermia), targeted drug delivery and biological labels.

1.6 Ferrites:

Ferrites are ceramic oxides holding iron oxide Fe_2O_3, as a major constituent [80-82].The history of ferrite materials can be found back to periods ago with the innovation of stones that fascinated iron. The naturally molded ferrite is magnetite (Fe_3O_4 or $FeO.Fe_2O_3$). The first man-made ferrites were industrialized independently in Japan and Netherlands in the 1930's. Since then, exhaustive efforts have been dedicated to this research area. It revealed significant signs of progress in both

science and technologies of ferrite materials. The exclusive electric and magnetic properties of ferrite materials to allow them to have an extensive range of applications, such as microwave components, magnetic fluids, high-frequency devices and magnetic data storage. Ferrites are mostly ionic and have very even crystal arrangement. Ferrites can be classified into three groups:

i. Spinel

ii. Garnet

iii. Magnetoplumbite.

The spinel-type oxides have the general formula AB_2O_4 where A is a divalent and B is a trivalent metal ion. The general chemical formula of spinel ferrites is $A^{II}\ Fe_2{}^{III}\ O_4$ where A^{II} represents divalent ions, as mentioned in Table 1.1.

Type	Structure	General Formula	Example
Spinel	Cubic	$A^{II}Fe_2O_4$	A^{II}=Fe, Cd, Co,Mg, Ni,Zn
Garnet	Cubic	$A^{III}\ 3Fe_5O_{12}$	A^{III}=Y, Sm, Eu, Gd, Tb,Lu
Magnetoplumbite	Hexagonal	$A^{II}Fe_{12}O_{19}$	A^{II}=Ba, Sr

1.6.1 Magnetic Properties of Spinel Ferrites:

According to the Neel's theory of ferromagnetism, ferromagnetic materials like cobalt ferrite ($CoFe_2O_4$) prepared of two sub-lattices (A and B). Contained by the particular sub-lattices, the magnetic moments are set parallel to one another but the strong interactions between the two sub-lattices outcomes in the anti-parallel pre-arrangement of the ordered moments in the two sub-lattices. A spinel ferrite then may be defined as the material which below a certain temperature (Curie temperature) shows a spontaneous magnetization, rising from the anti-parallel arrangement of the strongly coupled atomic dipoles [80-82].

1.6.2 Consequence of Spinel Ferrites:

Spinel ferrite of Nano-sized materials show remarkable electrical and magnetic properties and encouraging technological applications in different spheres of energy. The most inspiring feature

of Nanomagnetism is the custom of the nanomaterials in biological and clinical applications. Iron oxide is widely useful for several functions like cell separation and purification, contrast factor in magnetic resonance imaging (MRI), targeted drug delivery, magnetic fluids 33 hyperthermia (MFH) and Nano-biosensors. By using magnetic particles with affinity cancer cells, these cells can be selectively heated by an external alternating magnetic field in the range of 50-500 kHz frequency range. This heating result in the end of the selected cells, whereas the healthy cells are not affected by such discourse. The side effects of chemotherapy like 'hair loss' can be avoided [83]. Targeted drug delivery is a drug is attached to a magnetic carrier, directed by a magnet, can be produced to target a specific drug site. It helps in the local treatment of diseases in the uniformity with a more prey-specific delivery of drugs. Magnetic heating can also be used as a trigger to release drug from an implant. The drug is confined with a thermo-responsive polymer which releases the drug on its target when heated by means of an external AC-magnetic field [84].

1.6.3 Cobalt ferrite:

As an important member of the family of spinel ferrites, cobalt ferrite ($CoFe_2O_4$) centered materials have been putative as the encouraging candidates for a wide diversity of applications as well as magnetic and magneto-optical data storage due to their good chemical stability and magnetic properties such as the high Curie temperature, relatively high saturation magnetization and high magnetic anisotropy [83]. Also, among different metal ferrites, cobalt ferrite is known for its relatively high magnetostriction, and there have been many attempts to make sintered polycrystalline. Cobalt ferrite is categorized into a hard magnet due to its high corecivity and moderate magnetization. Due to its high magnetic corecivity value and good physical and chemical stability, it has been used for various applications.$CoFe_2O_4$ exhibits high coercive force, mechanical hardness, and chemical stability. The $CoFe_2O_4$ nanoparticles have received particular attention because of their slower magnetic moment relaxation compared to magnetite ones. Therefore, more efforts have been made for the synthesis and characterization of $CoFe_2O_4$ materials. The FCC structure of cobalt ferrite is shown in figure 1.6. It is composed of eight cobalt sites possesses tetrahedral coordination with oxygen and having 16 ferric sites having octahedral coordination.

1.6.3.1 Applications:

Cobalt ferrite nanoparticles possess a potential for possible future biomedical applications [83, 85] biosensing and Nanomedicine [86-88], spanning from cell separation, purification and contrast agents for magnetic resonance imaging [89] high-density magnetic devices [86, 90] Li+-batteries [91, 92], to drug delivery [93], biosensors [94], and magnetic fluid hyperthermia [95, 96].

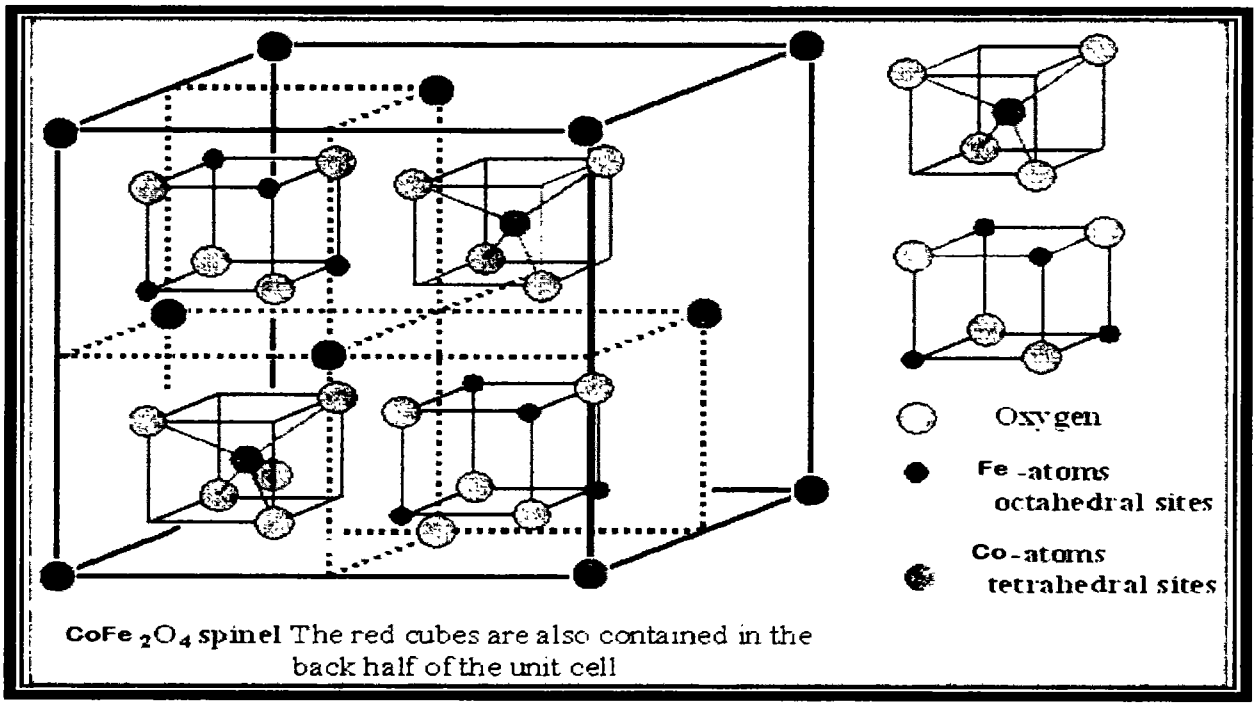

Figure 1.6: crystal structure of cobalt ferrite

1.7 Aims and objective:

The main objectives of this work are;

- To form stable and uniform sized mesoporous silica nanostructure by hydrothermal method and by using greener route
- Study on the formation and synthesis of cobalt ferrite coated mesoporous silica nanostructure ($Co.Fe_2O_4@SiO_2$)
- Study the effect of coating of cobalt ferrite on mesoporous silica nanostructure
- Surface characterization of ($Co.Fe_2O_4@SiO_2$) cobalt ferrite coated mesoporous silica nanostructure ($Co.Fe_2O_4@SiO_2$)
- Study applications of cobalt ferrite coated mesoporous silica nanostructure in drug delivery

Chapter No. 2

Synthesis Techniques

Introduction:

This chapter will describe the method adopted for chemical synthesis of cobalt ferrite coated on mesoporous silica nanostructure. Furthermore, different parameters have been examined to obtain high-quality nanoparticle with even distribution.

2.1 Synthesis of nanoparticles:

There are different techniques for the synthesis of nanoparticles, which are mostly grouped as top-down approach and bottom-up approach. In bottom-up approach, the single atoms get closer to each other to form large molecules. These approaches contain the contraction of materials components (up to atomic level) with further self-assembly progression leading to the formation. Top-down approach contains the decrease of bulk material of nanoparticle [97] as shown in figure 2.1.

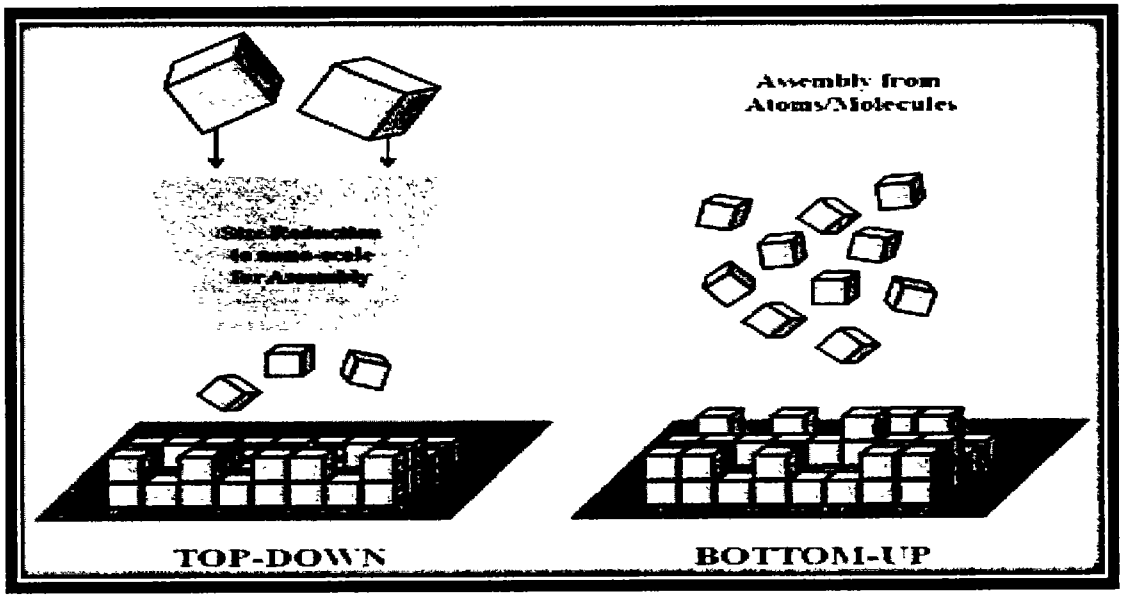

Figure 2.1: Schematic of synthesis of nanoparticles [97]

Chemical vapour deposition, sol-gel and DNA nanotechnology are a few examples of bottom-up approach while photolithography, Nanosphere lithography, and ball milling are a few good

examples of top-down approach [98]. Each approach is having its advantages and disadvantages. For example, in top-down approach by nature, aren't cheap and quick to manufacture - Slow and not suitable for large-scale production. Whereas in bottom-up start with atoms or molecules and build up to nanostructures. Fabrication is much less expensive when dimensions of nanostructure fall below nanometer scale then the bottom up is a better approaches compare to top-down approach because bottom-up approach enables one the yield nanostructure with less defect and more homogeneity. On the contrary, the top-down approach methods mostly create surface defects and contamination [99].

2.2 Synthesis of cobalt ferrite Nano particles:

In directive to obtain materials with the favored physical and chemical properties there are many techniques to synthesized the nanoparticles. The synthesis of cobalt ferrite nanoparticles through different method has become an essential area of research and development [100].Various methods of synthesizing spinel cobalt ferrite nanoparticles have been described, such as

- Ball Milling [101]
- Ceramic Method by firing [101]
- Co-Precipitation [101-103]
- Reverse Micelles [104]
- Hydrothermal Method [105, 106]
- Polymeric Precursor [107]
- Sol-gel [108]
- Micro Emulsions [109]
- Laser Ablation [110]
- Polyol Method [111]
- Sonochemical Approaches [112]
- Aerosol Method [113]

In this thesis, $CoFe_2O_4$ (cobalt ferrite) have been synthesized by "greener route"

2.2.1 Synthesis of cobalt ferrite Nano particles through greener route:

2.2.1.1 Plant used for the synthesis of cobalt ferrite Nano particles:

This biosynthetic method is modest and arranges for high-yield Nano-sized materials having well crystalline configuration and suitable properties. However, the high calcination temperature is necessary to renovate the precursor to form crystalline materials. Aloe Vera (Aloe barbadensis Mill) is a perennial succulent fit into the Liliaceal family, and it is a cactus-like plant that cultivates in hot, dry type of weather [114].

Figure 2.2: Aloe Vera Plant

For several years, aloe Vera has been testified to possess immunomodulatory, anti-inflammatory, UV protective, antiprotozoal, and wound- and burn-healing indorsing properties [115,118].

2.2.1.2 Preparation of plant extract:

The solution of Aloe Vera plant extract was prepared by using 5 g slice of carefully washed Aloe Vera leaves. We cut Aloe Vera leaves magnificently and got Aloe Vera gel. The obtained gel was dissolved in 10 ml of de-ionized water then stirred for 30 min to attain a clear solution. The resulting product was used as an Aloe Vera plant extracted solution. The whole process of preparation of aloe Vera plant extract solution is shown in figure 2.3.

2.2.1.3 Chemicals:

These chemicals are used in the preparation of cobalt ferrite nanoparticles. Table 2.1. Chemical used in preparation of cobalt ferrite nanoparticles.

Chemicals	Chemical formula	Chemical Structure
Cobalt nitrates	$Co(NO_3)_2$	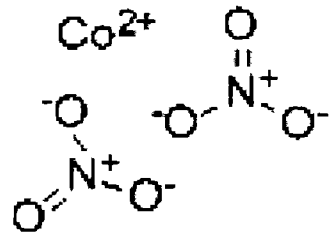
Ferric nitrate	$Fe(NO_3)_3$	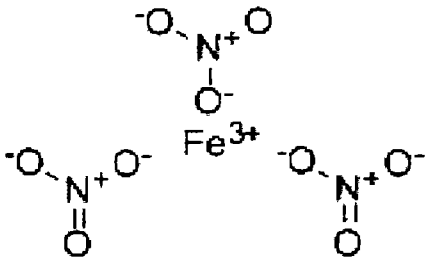
Ethanol	C_2H_6O	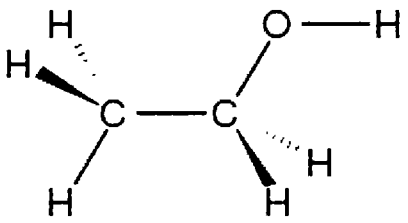

Deionized water	H_2O	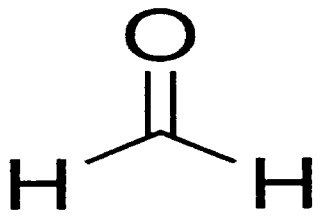

2.2.1.4 Process for the preparation of cobalt ferrite Nano particles:

By using Co-Precipitation method, we synthesis cobalt ferrite. At room temperature Ferric nitrate and cobalt nitrate is dissolve in Aloe Vera plant extract solution under vigorous stirring for 1h. As a result of stirring a clear solution was gotten. Then precursor mixture of metal nitrates in Aloe Vera extracted solution was retained in domestic oven for 10 min. when solution reached at the point of spontaneous combustion it vaporizes and rapidly become solid. After completion of the reaction obtained solid powder was washed and dried.

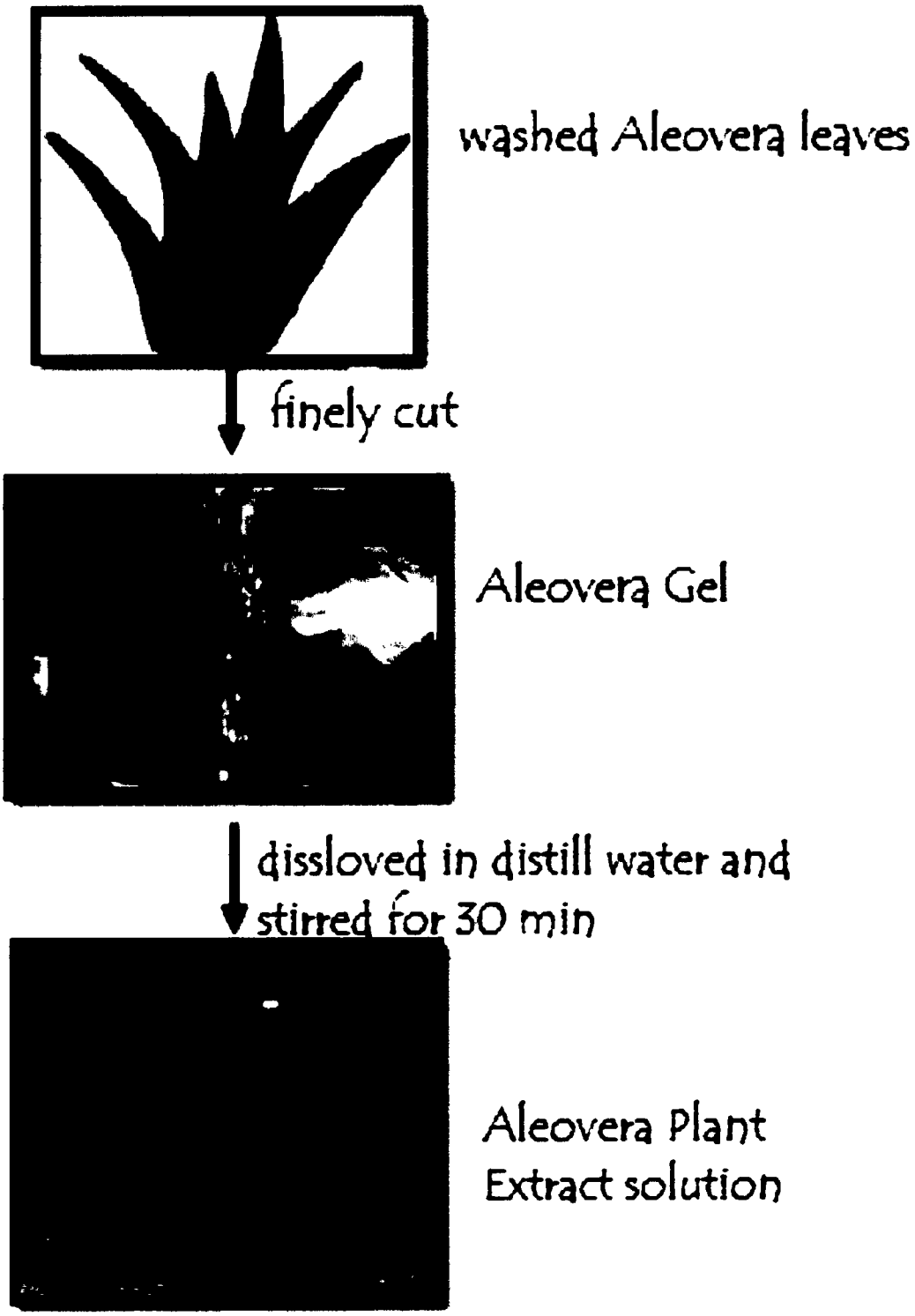

Figure 2.3: Schematic Diagram of preparation of plant extract solution

2.3 Synthesis of mesoporous silica Nano particles:

The properties of nanoparticles are highly size-dependent so the synthesis of nanoparticles with desire size is of great importance. The different route has been developed for the synthesis of mesoporous silica nanoparticles. Some of these are dry methods (solid state method) and some are wet methods (chemical method). In the dry method, the primary products are mixed directly and then heats. In the wet chemical method, the primary solutions of the salt are mixed together and then dried at a certain temperature.

The wet methods of preparation of mesoporous silica are as follows:

- Chemical Co-Precipitation [119]
- Vapor-Phase Synthesis [120]
- Hydrolysis [121-123]
- Microemulsion method [124]
- Thermal treatment method [125]
- Sol-gel method [126, 127]

In this thesis, mesoporous silica nanoparticles have been synthesis by chemical hydrothermal method and greener route.

2.3.1 Chemicals:

These chemicals are used in the preparation of mesoporous silica Nanoparticles through chemical route as shown in Table 2.2.

Chemicals	Chemical formula	Chemical Structure
Pluronic P-123	$HO(CH_2CH_2O)_{20}(CH_2CH(CH_3)O)_{70}(CH_2CH_2O)_{20}H$	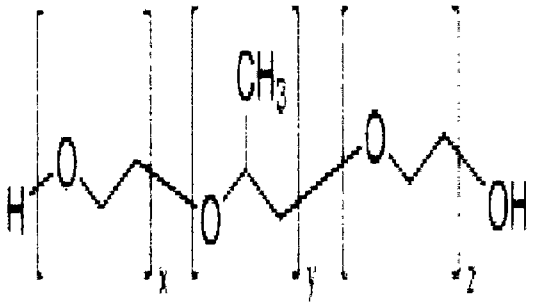

Cetrimonium bromide CTAB	$C_{19}H_{42}BrN$	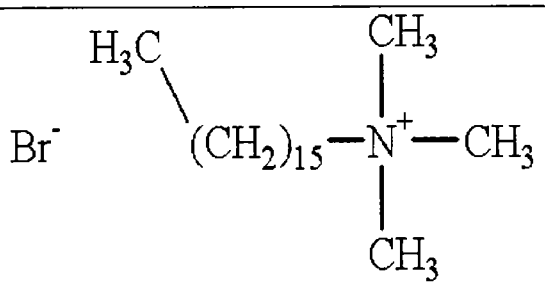
Tetraethyl orthosilicate TEOS	$SiC_8H_{20}O_4$	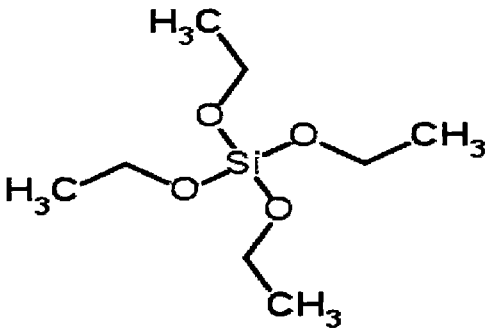
Ethanol	C_2H_6O	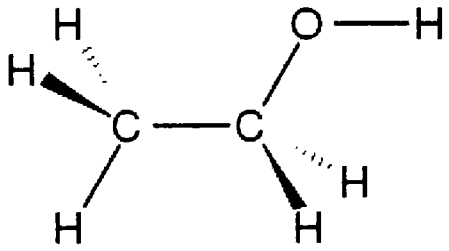
Deionized Water	H_2O	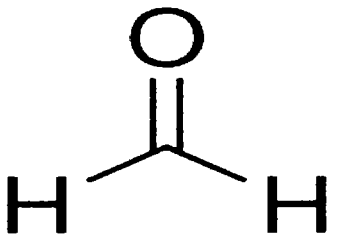

2.3.2 Preparation of mesporous silica Nano particles:

A solution made by mixing of 60 ml of 2M HCl, 30 ml H_2O, and 25 ml ethanol. Then add 3 g of triblock copolymer P123 and 0.5 g of CTAB dissolve. Under magnetic stirring, 10 ml of TEOS was added to the aqueous solution at room temperature. After 30 min of stirring, the solution was transferred into a Teflon-lined steel Parr autoclave and heated at 80°C for 5 h, and then retained at

a higher temperature (120 or 130^{0}C) for 12 h. The white precipitate was collected and dried at 90°C for 24 h. For the removal of templates, the sample was calcined at 550°C for 5h.

2.3.3 Process for the coating of cobalt ferrite on mesoporous silica Nano particles:

First, 1.5 g of silica (through chemical route) was dissolved in 10 ml of ethanol. In another beaker, 0.5 g of cobalt ferrite was dissolved in 10 ml of ethanol. When both samples were dissolved in ethanol then put these beakers in the sonication bath for sonication. After 30 min, samples completely dispersed in ethanol. We mixed both suspensions and stirred for 1 h. then the powder is collected by centrifugation and dried at 90°C.

2.4 Synthesis of mesoporous silica Greener route:

2.4.1 Plant used for synthesis of mesoporous silica Nano particles by greener route:

Azadirachta indica- Neem plant is the most extensively obtainable and fast growing plant. It is most usually used the old-fashioned pharmaceutical plant. Significant development has been made in estimating the biological activity of phytochemicals for medicinal applications. The phytochemicals present in Neem plant efficiently act as plummeting and capping agent. In the modern era, Neem is reflected as an appreciated source of exclusive natural products for improvement of medicines against *numerous diseases [16,128,129].*

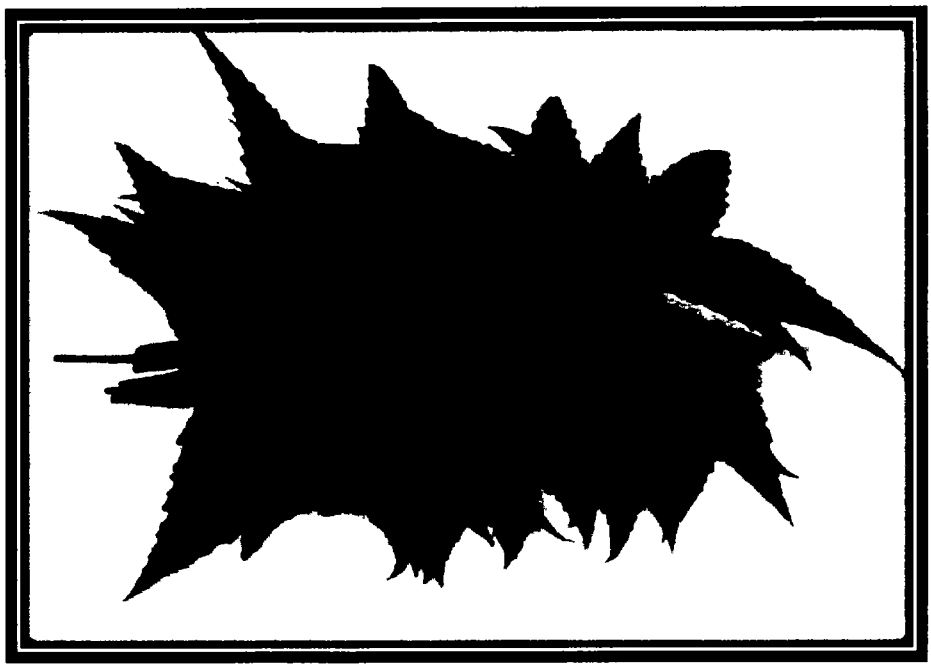

Figure 2.4: Neem leaves

2.4.2 Preparation of plant extract:

Firstly the Neem leaves were washed with tap water so that to remove all the dust. For further removal impurities, the leaves were washed with distilled water. After washing the leaves were air dried. By using mortar and pestle air dried leaves were crushed and grinded. The crushed and grounded pastes of leaves were boiled in 200 ml of distilled water for 10-15 minutes until bubbles appear in the mixture. The filtration was completed in two steps. The leaves paste was filtered using filter paper. The filtrate then obtained was the required plant extract of Neem plant.

2.4.3 Chemicals:

These chemical are used in the preparation of mesoporous silica through greener route are in Table 2.3.

Chemicals	Chemical formula	Chemical Structure
Cetrimonium bromide CTAB	$C_{19}H_{42}BrN$	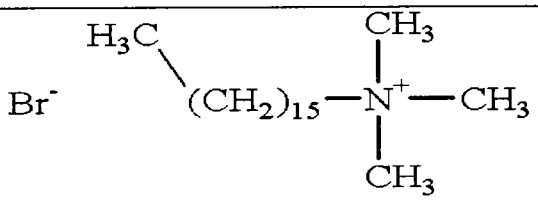
Tetraethyl orthosilicate TEOS	$SiC_8H_{20}O_4$	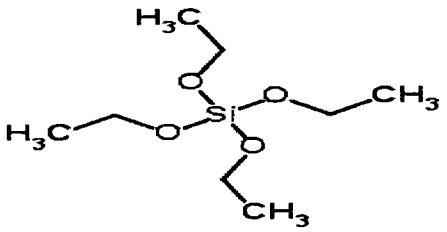
Ethanol	C_2H_6O	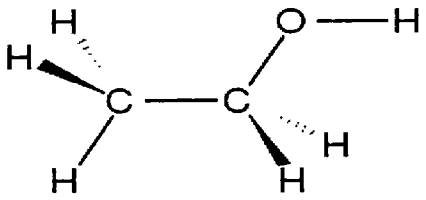
Deionized Water	H_2O	

2.4.4 Preparation of mesoporous silica Nano particles through greener route:

For the green synthesis of mesoporous silica nanoparticles 1:1 amount of silica precursor TEOS and Neem plant extract bit by bit mixed together with slight heating and stirring. The ethanol CTAB solution (1:0.1) solution was added to the foregoing mixture. During the process, 50-60°C temperature and magnetic stirring were given overnight. The next day supernatant was decanted and the particles were dried in drying in the oven at 60^0C temperature. The green synthesized NPs were then washed with distilled water 4-5 continuous washings were given to the NPs. During the washing process distilled water was added to the NPs and stirred using magnetic stirrer and then allowed to settle. After 15-20 minutes the NPs got settled in the bottom and the supernatant was decanted. After the washing, the NPs are dried in drying oven at 60°C temperature. The mesoporous silica nanoparticles were calcined at 500°C for 5 hours. Calcination purifies and removes volatile impurities from NPs.

2.4.5 Process for the coating of cobalt ferrite on mesoporous silica Nano particles:

First, 1.5 g of silica (through chemical route) was dissolved in 10 ml of ethanol. In another beaker, 0.5 g of cobalt ferrite was dissolved in 10 ml of ethanol. When both samples were dissolved in ethanol then put these beakers in sonicate bath for sonication. After 30 min, samples completely dispersed in ethanol. We mixed both suspensions and stirred for 1 h. then the powder is collected by centrifugation and dried at 90°C.

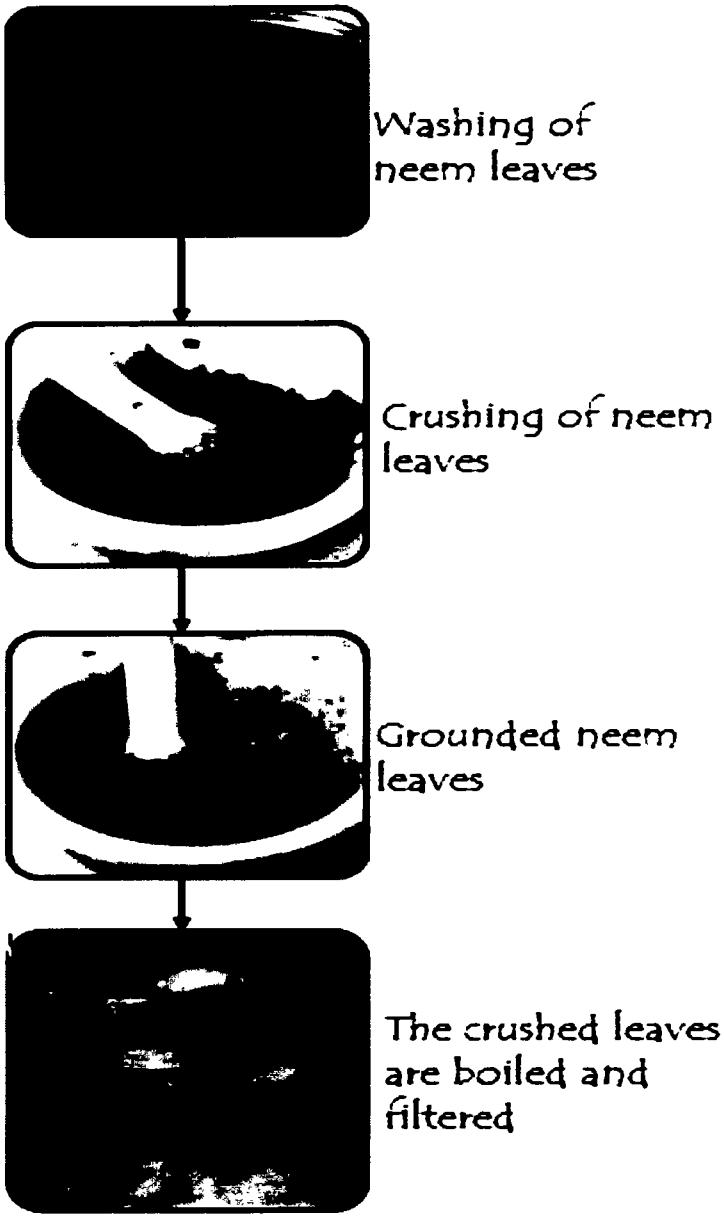

Figure 2.5: Schematic Diagram of preparation of Neem plant extract solution

2.5 Applications:

In this work, we have used mesoporous silica as a Nanomedicine, because mesoporous silica nanoparticles is honey-comb like structure with empty channels to encapsulate compounds. We choose Ketoprofen as a model drug. Ketoprofen is used to dismiss pain from various circumstances. It also diminishes pain, swelling, and joint stiffness from arthritis. This medication is a nonsteroidal anti-inflammatory drug (NSAID). It works by blocking your body's production of certain natural substances that cause irritation. This consequence helps in Reduction of swelling, pain, or fever.

2.5.1 Drug loading:

0.5 gm of Ketoprofen was dissolved in 10 ml of ethanol. In the drug solution, 0.5 gm of mesoporous silica nanoparticles were added. Then the suspension for 2h while the evaporation of ethanol is avoided. After stirring it was centrifuged and air dried to get drug loaded nanoparticles. Filtrate (1.0 ml) was take out with vital and diluted to 100 ml and then was analyzed by UV/VIS spectroscopy at a wavelength of 265nm.

2.5.2 Drug release:

The release pattern was perceived in PBS buffer (pH= 7.4). Drug loaded particles were diverse in PBS and kept in 37° shaking bath for 30 minutes. After 30 minutes the particles were centrifuged and optical density of particles is checked at 265 nm by using UV- Visible Spectrophotometer.

Chapter No. 3

Characterization techniques

Introduction:

Every material has its own particular properties. Different techniques can be used to fathom the properties of nanoparticles. Each technique gives some specific information; some are allied to chemical and others may be associated with physical properties. Different tools of characterization have been used to study structural and chemical properties of materials.

- X-Ray Diffraction
- Scanning electron microscopy
- Energy dispersive X-Ray spectroscopy
- Fourier transform infrared spectroscopy

3.1 X-ray Diffraction (XRD):

X-Ray Diffraction (XRD) is an effective and non-destructive technique that is used to study structural parameters such as crystalline structures, crystal size and other crystallographic information [130, 131].

3.1.1 Working principle of X-ray diffraction:

When x rays are incident on a set of equally spaced parallel planes of distance 'd' apart then these are reflected ray having to a path difference of $2d\sin\theta$, where θ is angle between incident ray diffracting plane of crystal as shown in figure 3.1 [132]. Diffraction peaks appear only if different reflected rays are in phase and constructively interface. Otherwise no diffraction pattern can appear [133]. If λ is the wavelength of the incident beam then the path difference for constructive interference is given by Bragg's law as [134].

$$\textbf{Path difference} = n\lambda = 2 d_{hkl} \sin\theta_{hkl} \qquad 3.1$$

Where n is an integer.

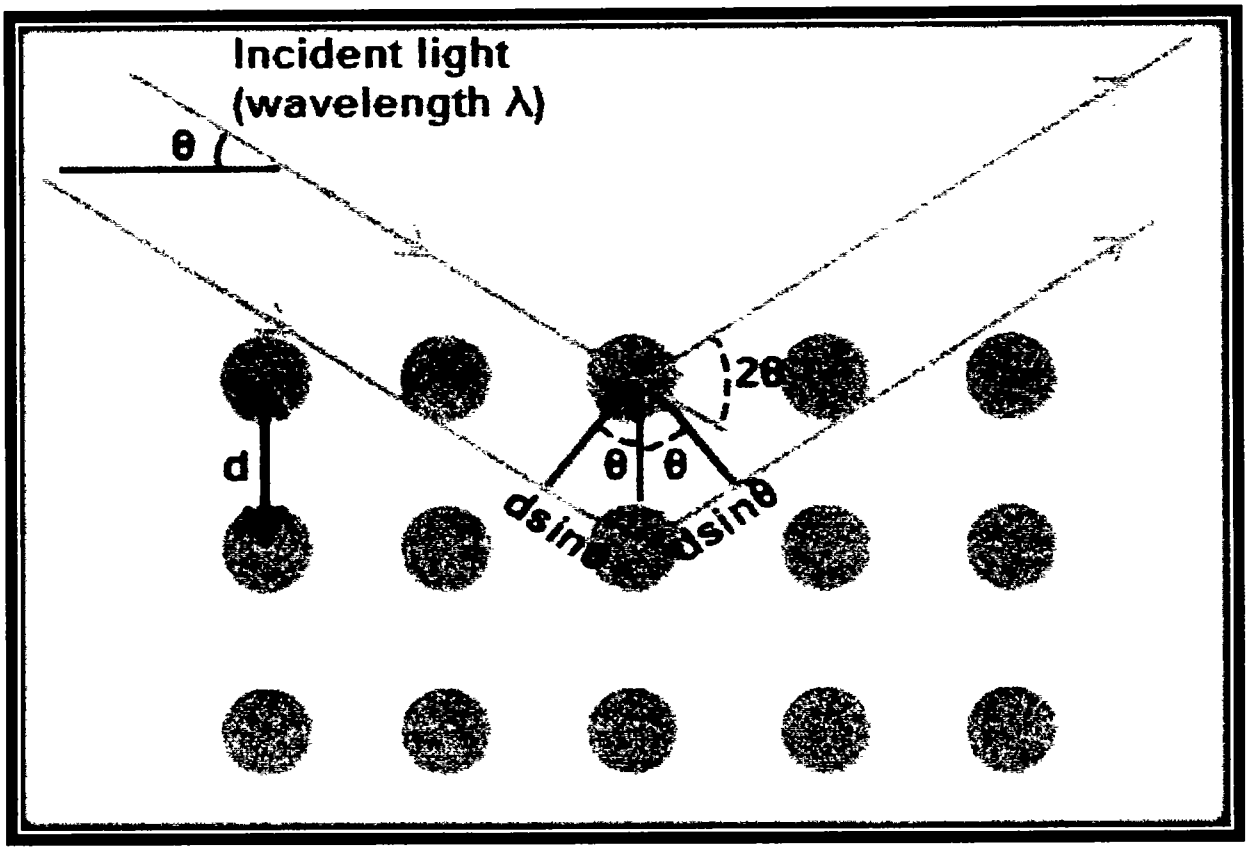

Figure 3.1: Schematic diagram of diffraction by atomic planes of crystal [132]

Three different methods can be used on the basis of brag's law to have diffraction from crystal [131].

- Laue method
- Rotating crystal method
- Powder diffraction method

Mostly powder diffraction technique is used in this project. Therefore, only this technique will be discussed in detail.

3.1.2 Powder diffraction method:

The sample in powder form is exposed to monochromatic x rays of known wavelength. The sample in powder form consists of a number of crystallites having a number of random distributions of orientation with respect to incident X-ray beams. Some particles will be oriented in a way. For example, Bragg's reflection will occur by their (1 1 1) planes. Other particles will be rightly oriented for oriented for reflection by (1 0 0) planes and so on.

As a result, each of the sets of lattices planes in the crystal is capable of satisfying Bragg's angle of reflection with the incident beam. In this method, no actual rotation of the crystal system occurs but the distribution of the number of crystallites in every possible direction is equaling to single rotted about all possible direction of 2 θ [131, 133].

3.1.3 Particle size:

The term particle size is used to refer crystals having size lesser than 1000 angstrom. The average size of the particle is estimated by Scherrer formula from the broadening of diffraction peaks.

$$t = \frac{0.9\,\lambda}{\beta \cos\theta} \qquad 3.2$$

Where t is a size of crystallite, λ is the wavelength of incident radiation and beta is full width at half of its maximum intensity (FWHM) shown in the figure 3.2. Beta is calculated in radians and roughly it can be measured as:

$$\beta = \frac{1}{2}\,(2\theta\,a - 2\theta\,b) \qquad 3.3$$

Broadening of peaks is mostly considered due to particle size effect. It is used to calculate the particle size of loose powders instead of individual crystal size in a solid mass. The Width of diffraction curve and particle size is inversely proportional to each other as shown in fig [131].

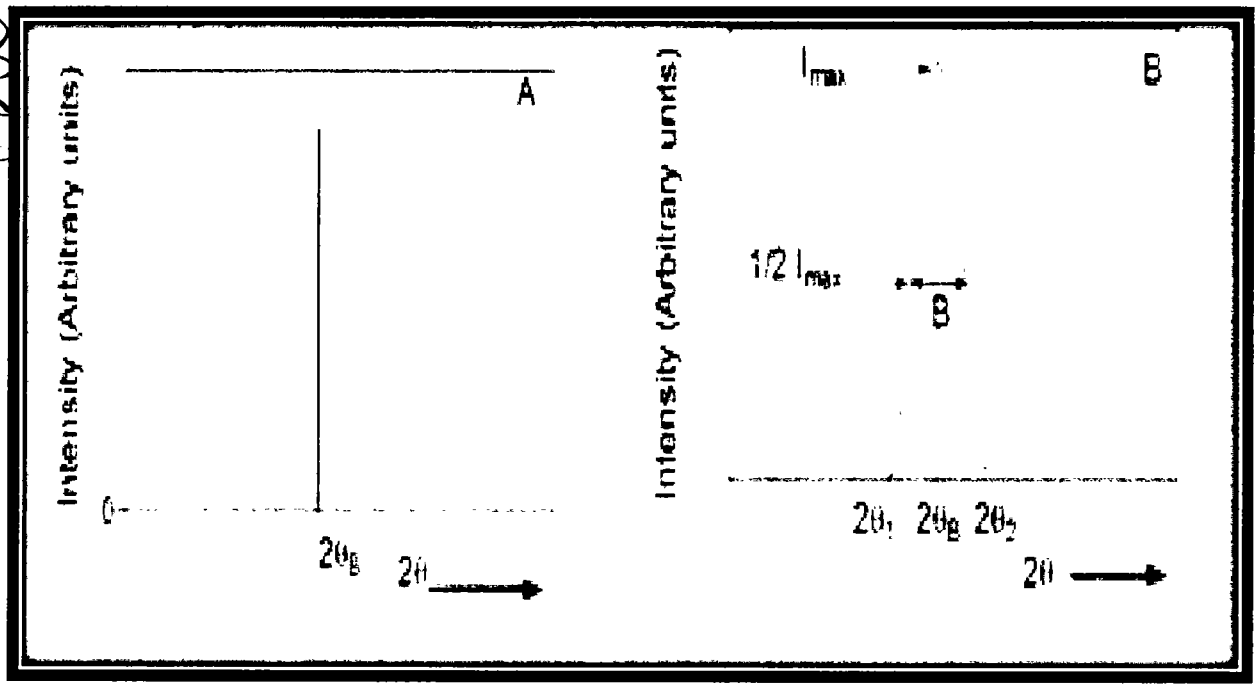

Figure 3.2: Schematic diagram of effect of particle size on diffraction curve [135]

3.2 Scanning electron microscopy:

Scanning electron microscopy (SEM) is most commonly used mapping technique [136]. In typical SEM, the sample is scanned by a focused beam of accelerated electrons. These electrons are produced by field emission or thermionic source. These electrons are accelerated with energy 500eV to 50KeV [137]. The interaction of electrons with the surface of samples produced a number signal as shown in figure 3.3. These signals are

- Secondary electron (SE)
- Backscattered electrons (BSE)
- Transmitted electrons
- Reflection High-Energy electron diffraction (RHEED)
- X-Rays
- Auger electrons
- Cathodoluminescence (CL)
- Electron beam induced current (EBIC) [135]

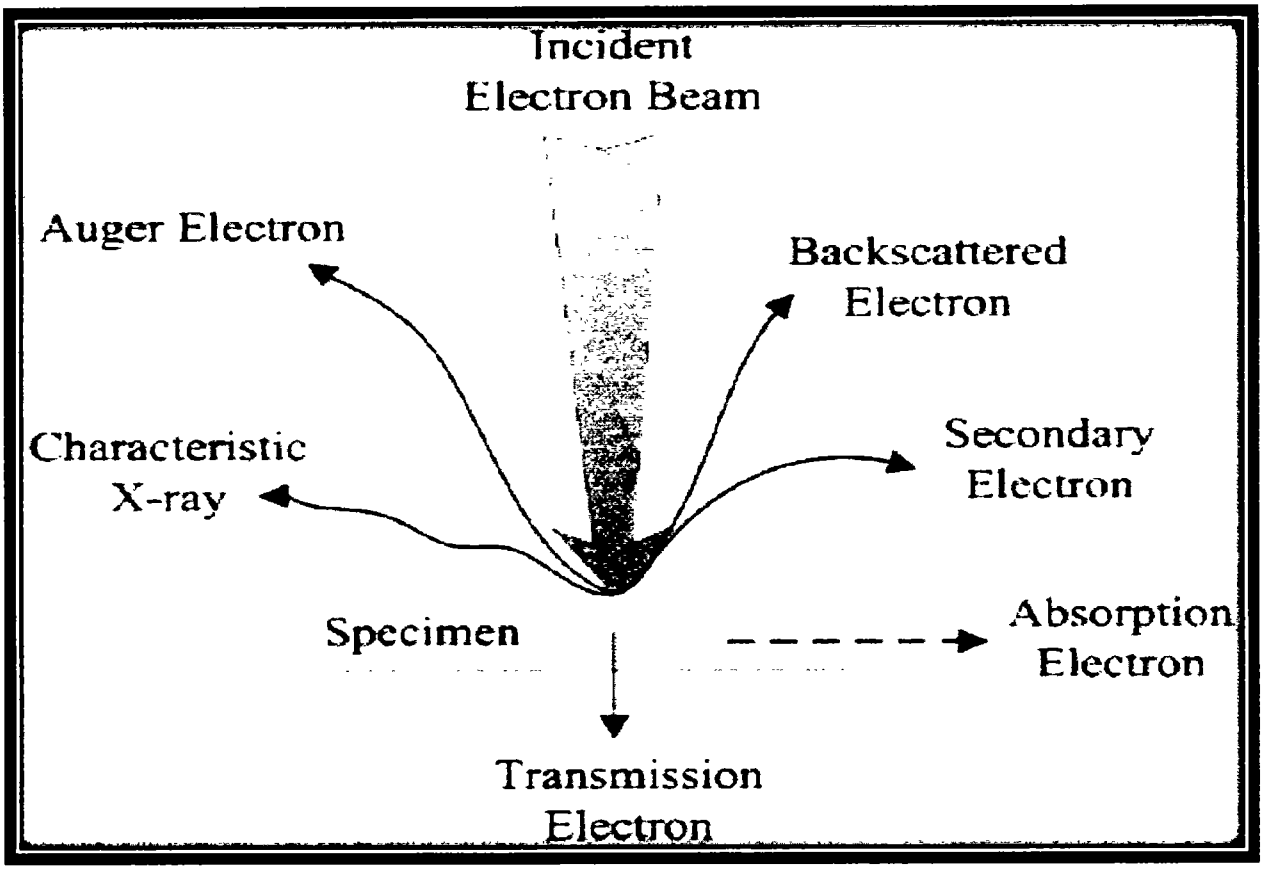

Figure 3.3: Schematic diagram of SEM principle [138, 139]

SEM has different modes of operation based upon the type of signal. Secondary electron imaging is most commonly used. Secondary electrons are emitted by the sample under inelastic scattering of the incident electrons with nucleus or electrons of the atom respectively. The energy of secondary electrons lies in the range of 0-50 eV. Information about surface chemistry, morphology and topography can be obtained very easily at a spatial resolution of 1nm. Backscattered electron (BSE) are highly energetic electron with energy 50 eV to the energy of incident beam [136, 138].The number of BSE varies as a function of atomic number (Z) of the sample material. The BSE imaging is employed as Z- contrast imaging. These electrons suffer diffraction and come from inside of material so these are used to study interior bulk crystallographic information. In X-Ray mapping and the interaction of incident electromagnetic radiation with the specimen atoms causes the ejection of inner shell electrons. As a result in order to get back to ground state, atoms either emit characteristic X-Rays by the transition of high shell electrons to vacant inner shells or by the emission of Auger electron. Both of these give quantitative as well as quantitatively information about chemical composition of the specimen. This procedure is the basis of energy dispersive X-Ray (EDX) spectroscopy or X-Ray micro-analyzer [136, 138].

For the current research purpose, SEM provided with EDX setup is employed in secondary electron imaging mode for morphological, microstructural as well as elemental analysis of synthesized silica and cobalt ferrite samples.

3.3 Energy dispersive X-Ray spectroscopy:

Energy dispersive X-Ray (EDX) spectroscopy is a fast and fast and non-destructive technique used for the elemental or compositional analysis of every kind of sample having atomic number 4 (Be) to 92(U) . This technique gives both qualitative and quantitative analysis of the material. The working principle of this technique is shown in fig 3.4.

The atoms of the material are exposed to X-Ray of short wavelength as an excitation and ionization of atoms occur. These incidents X-Ray photons knock out the tightly bound electrons of inner shells. In order to fill the vacancies, the electrons from outer shells move to inner shell by releasing energy in the form of photons. This energy is equal to the difference between two shells.

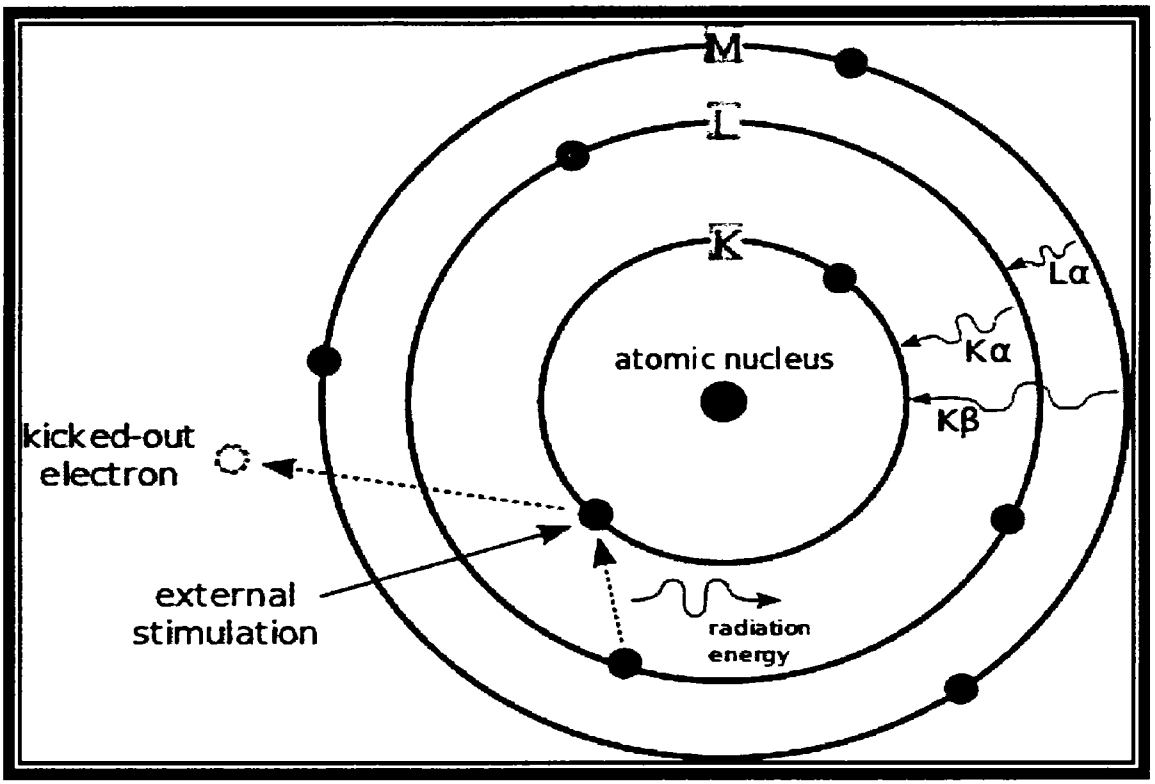

Figure 3.4: Schematic of EDX spectroscopy principle [140]

The energy emitted by a transition of electrons is smaller than the energy of primary X-Rays. Every element of the periodic table has its own electronic configuration so the energy of emitted X-Rays is the characteristic of each atom. The emitted X-Rays can be detected and converted into intensity versus energy spectrum. The position of peaks in the in the spectrum shows the elements present in it. The height of the peak gives the amount of the elements present in the sample.

In the current research work EDX spectrometer provided with SEM is used for the compositional analysis of silica coated cobalt ferrite nanostructure sample.

3.4 Fourier transform infra-red spectroscopy:

The crystal is made up of atoms or ions which are bonded to each other by chemical bonds. These atoms or ions can be put into vibration regarding one another above absolute temperature. The frequencies of these vibrations are dependent upon atomic weight and bond strength of the atoms. These vibrations occur at very high frequencies lying in infra-red part of electromagnetic spectrum. When material are exposed to electromagnetic radiation, the exchange energy occurs by resonance process. The absorption of energy occurs only in a discrete manner. As a response to energy absorption, the molecule gets shifted to the excited state of their vibrations. Molecules possess two

types of vibrations which are stretching and bending. The absorption of energy can be expressed in the form of radiation spectra which is plotted between wave number and absorption or transmittance intensity. Due to the combination of vibrational and rotational motion, the energy bands are observed instead of discrete energy lines.

FTIR is an advanced analytical type of technique which is accurate, speedy and non-destructive. The interaction of sample and infrared radiation occurs in the form of absorption, reflectance or transmission of Irradiation [141]. Since every bond has its own characteristics set of vibration frequencies in IR region. The recorded spectra of molecular absorption or transmission give the fingerprint of each component of material [141]. FTIR spectroscopy is not only used to detect organic but also the inorganic unknown material of any form such as liquid, solid and gasses. Moreover, this technique can also use to find the quality of the sample by giving a quantitative analysis of every component present in the sample [142].

Consider "I_o"and"I" be the intensity of incident radiation and the light beam after it has interacted with the sample material, respectively. The fundamental objective of FTIR technique is to find intensity ratio I/I_o versus frequency plot. The IR spectrum can be obtained in any of transmittance, reflectance and absorbance modes.

In case of reflectance,

$$R_\omega = (I/Io)_\omega \qquad 3.10$$

Where "R_ω" is the reflectance of the sample at the frequency ω and I_r is the intensity of reflected light. In the case of transmittance, the ratio is equated as T_w with I_r being replaced with I_t (intensity of transmitted light).

In the case of absorbance,

$$A_\omega = -\log T_\omega \qquad 3.11$$

Where A_ω is the part of light absorbed in the sample above expression is known as **Beer –Lambert Law.**

3.5 Absorption spectroscopy by UV spectrophotometer:

Visible or ultra-violet light is immersed by molecules such that beam is reduced as well as absorbed quickly. Hence, absorbance is found to the proportional to amount of reduction.

Radiation is absorbed for that specific value of frequency for which the difference in energies among two quantum mechanical states of molecules matches with each other. According to Beer's

law, absorbance increase with an increase with an increase in path length and amount of species that absorb light.

Mathematically,

$$A=ebc \qquad 3.12$$

Here A stands for absorbance, b denotes path length, c is the intensity of absorbing molecules and e is proportionality constant, known as absorptivity. Visible light has an extensive range of wavelengths, molecules react to these wavelengths quite inversely. A molecule can have many structural groups in itself and these structural groups stimulate different absorption bands in the spectra [143].

Whenever a beam of light is absorbed by a molecule, electrons in the outermost shell of the atoms are excited to higher energy states. Whether the light is visible or ultraviolet, electrons absorb energy and move from ground to excited states. Atoms move in the molecules with respect to each other atoms, they do not remain stationary. Their movement may be in the form of vibration or rotation. Discrete energy states are induced due to such vibration or rotation, these energy states lie above each other [144].

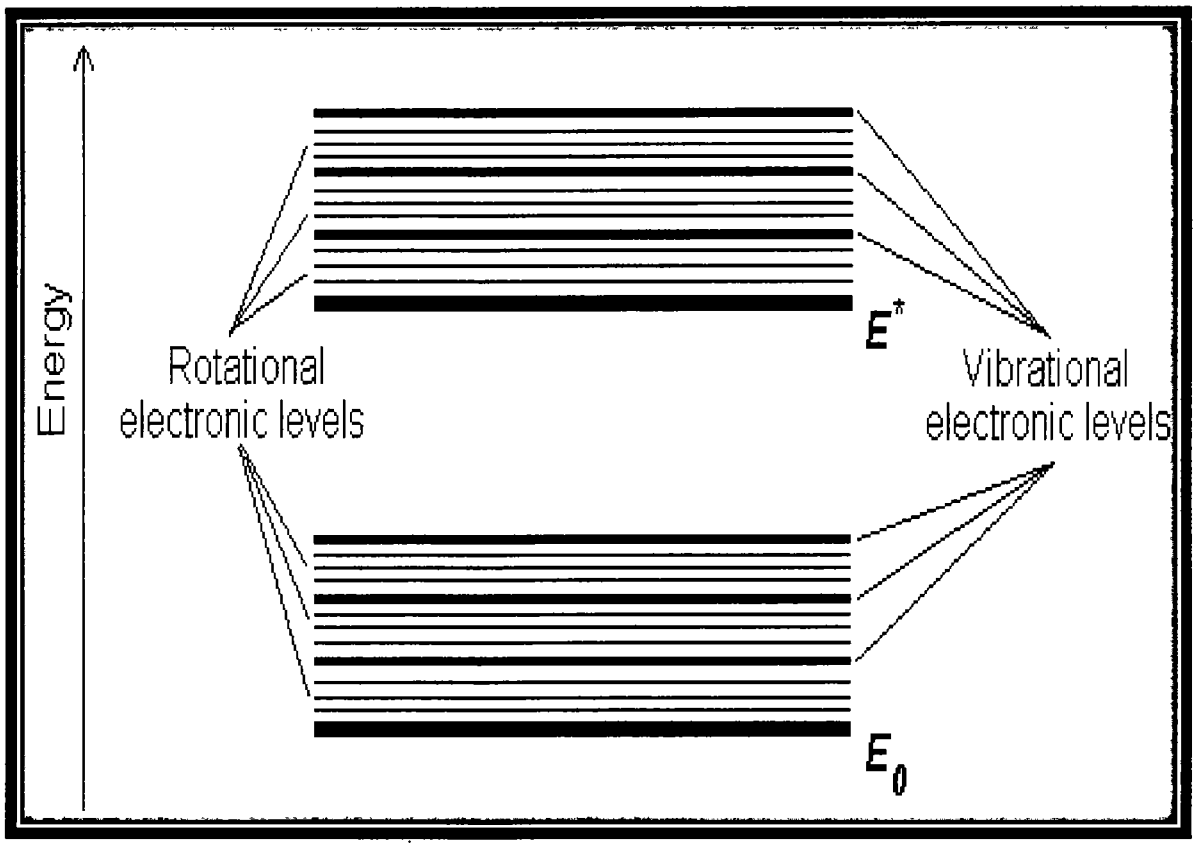

Figure 3.5: Discrete energy levels corresponding to radiations and vibrations [145]

There are three types of electron shells in which valence electrons reside:

1. Orbital with single bond called σ bonding orbital.
2. Orbital in double or triple bonding state i.e. as πbonding orbital.
3. Orbital having lone pair of electrons i.e. not –bonding orbital.

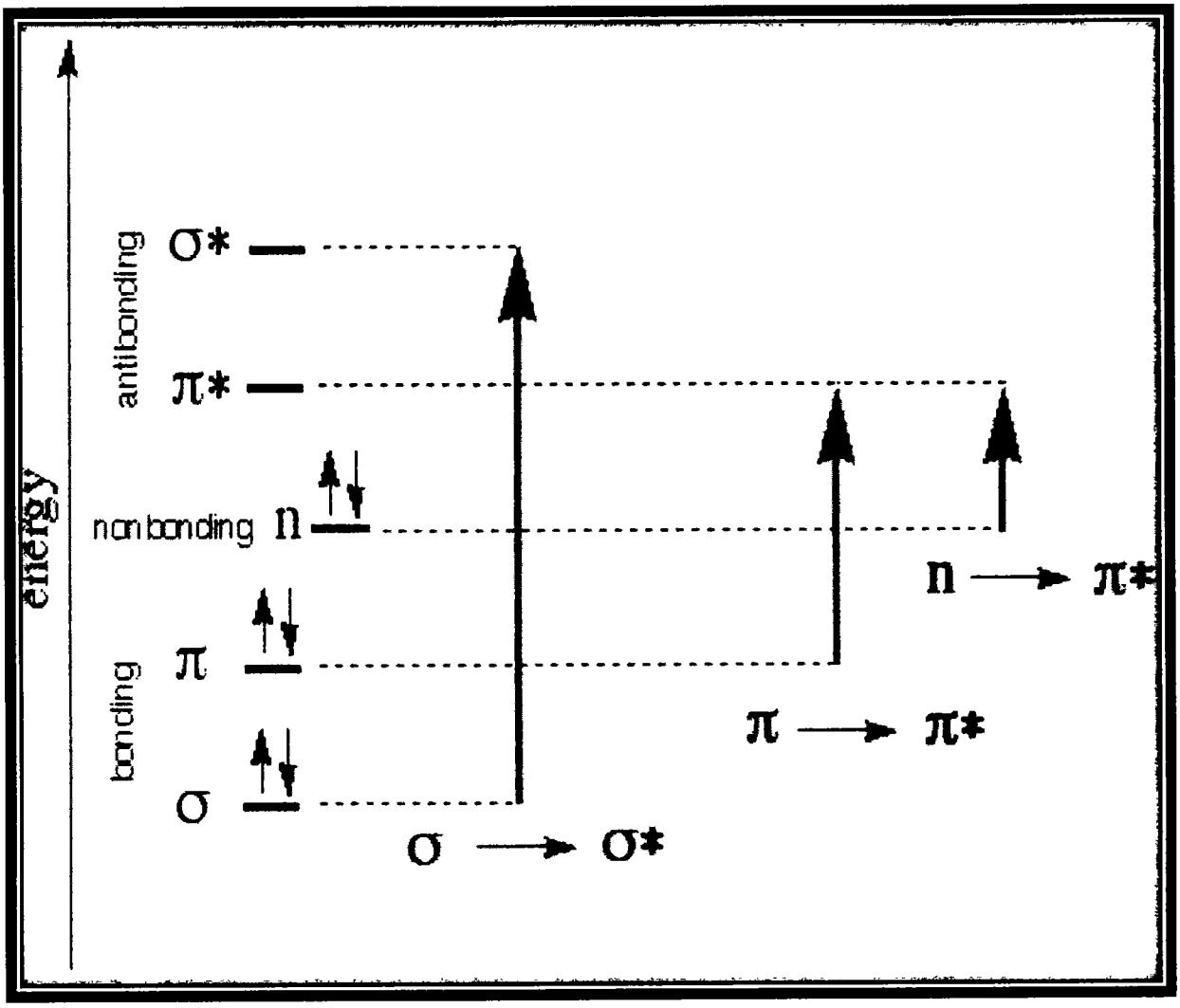

Figure 3.6: electron transition in ultraviolet/visible spectroscopy

In a typical spectrophotometer, a square shaped sample holder carries a sample from which an electromagnetic radiation passes. This sample holder is typically 1cm wide sample is subjected to electromagnetic radiation for 30 seconds. These electromagnetic waves belong to the whole ultraviolet range of the spectrum. A reference cell which contains a solvent is simultaneously subject to the radiation of the same intensity and frequency. Radiation that is transmitted from both, the sample and the reference cell are detected by the photocell.

Then spectrometer makes a comparison between intensities of radiations passing through both objects. The absorption spectrum is finally compiled by the computerized system. Modern spectrometers can simultaneously monitor the radiation chart. [144]

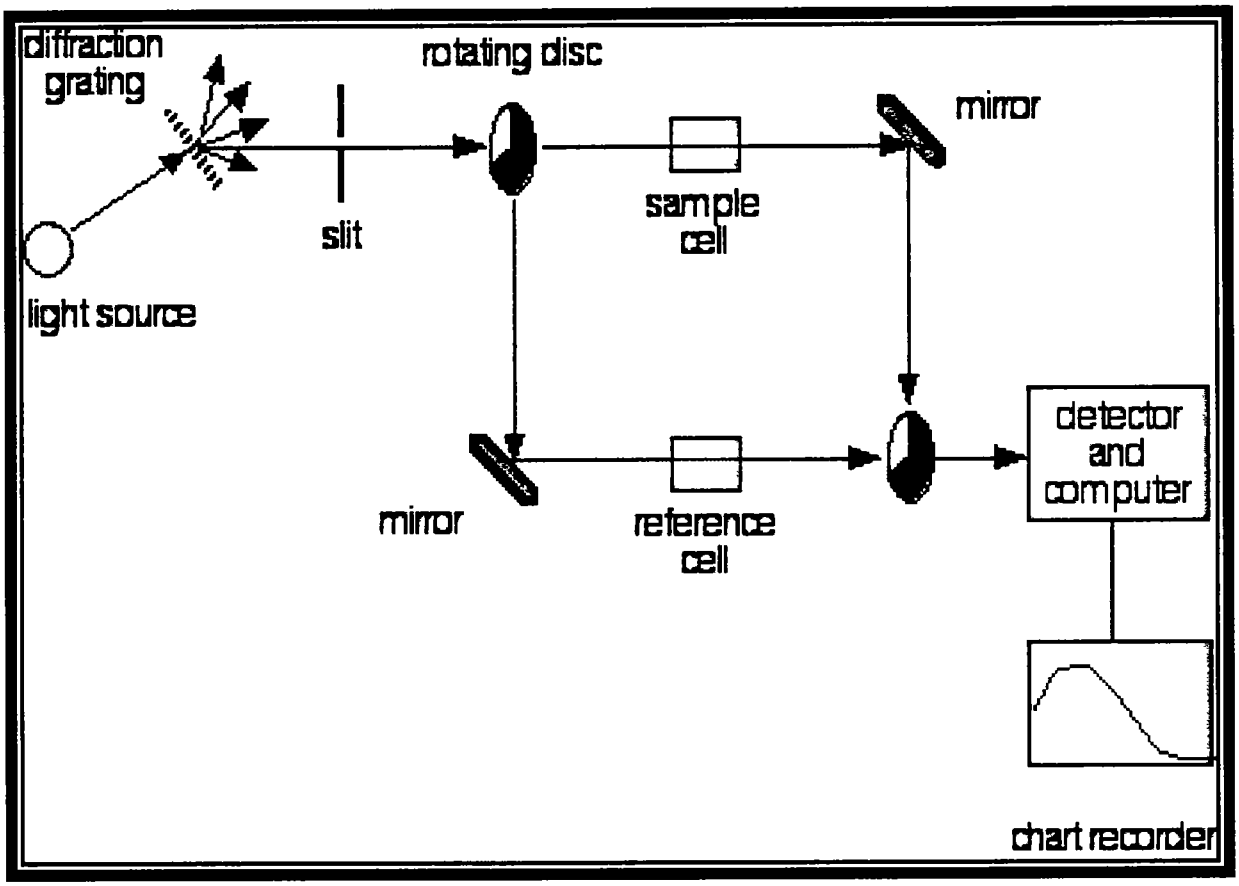

Figure 3.7: Working of UV/Visible Spectrophotometer

Chapter No.4

Results and Discussion

Structural investigation:

4.1 X-ray diffraction studies:

4.1.1 XRD analysis of Cobalt ferrite Nano particles prepared from greener route:

The X-Ray powder diffraction (XRD) Pattern below also endorsed the growth of cobalt ferrite. The peak in the diffractogram was same as the predictable samples peaks for cobalt ferrite which known in the JCPDS database and related literature [146]. The XRD pattern clearly shows that the prepared sample of cobalt ferrite nanoparticle was absolutely of the cubic spinel structure. A close inspection of XRD patterns discloses that the diffraction peaks are sharp, which is the indication of Nano crystallinity.

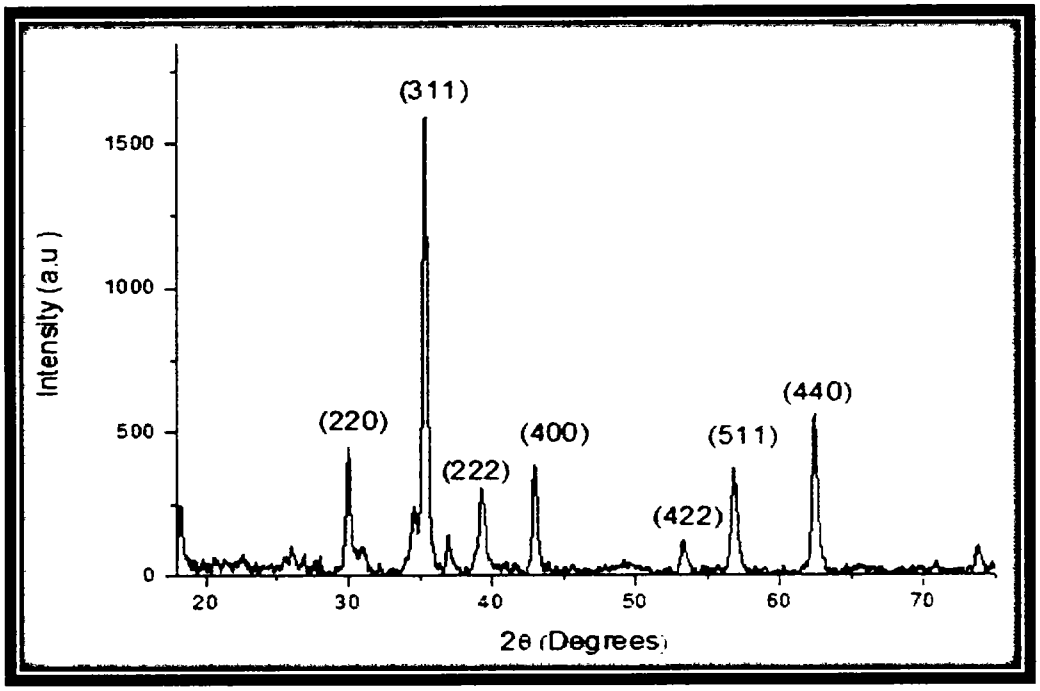

Figure 4.1:XRD pattern of cobalt ferrite [146]

4.1.2 XRD analysis of Mesoporous silica nanoparticles prepared from greener route:

The X-Ray powder diffraction (XRD) Configuration below sanctioned the formation of mesoporous silica. The XRD results shows the nature of silica is amorphous and a characteristic wide halo peak at $2\theta = 20^0$ [147, 148]

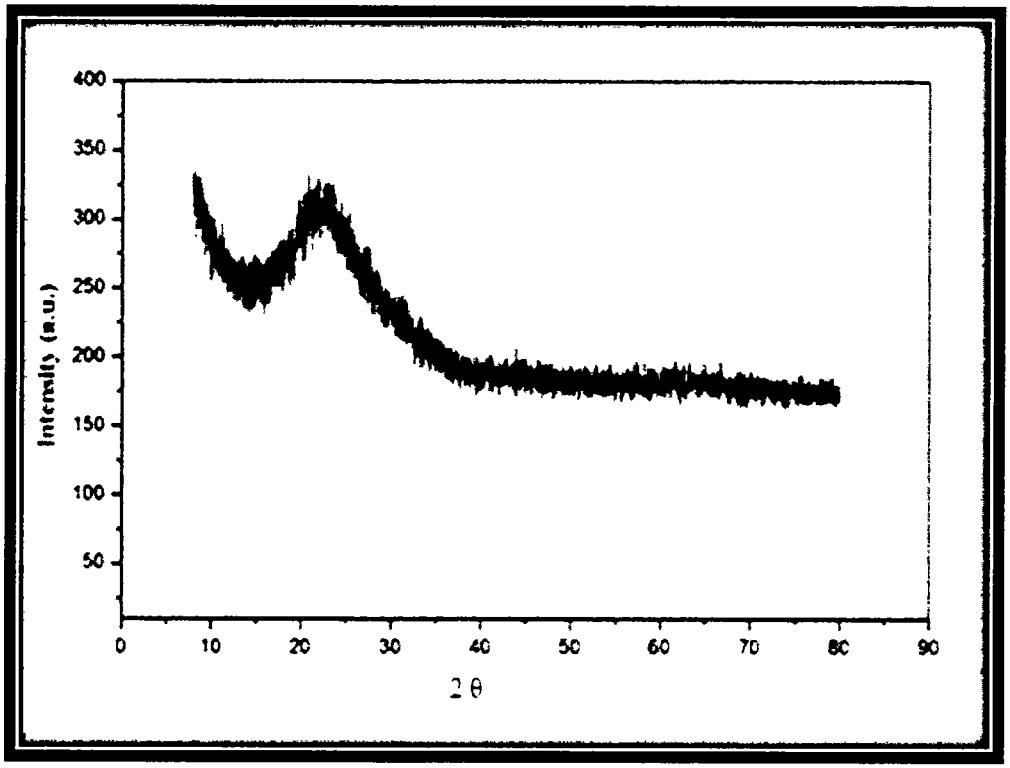

Figure 4.2: XRD pattern of mesoporous silica from greener route

In figure 4.3 shows the XRD result of mesoporous silica nanoparticle from the hydrothermal route. This shows that it has a wide-angle X-ray diffraction pattern of the mesoporous silica nanoparticle which has a characteristic peak of amorphous mesoporous silica at $2\theta=23.3^0$.Yang et al [149] synthesized silica nanoparticles indicated a characteristic peak at $2\theta=23^0$. Zhang et al. [150] also noted one widened XRD peak for amorphous silica centered at a 2θ value that is close to our measurement. Chen et al [151] approved that x-ray diffraction result of mesoporous silica were amorphous silicon dioxide having 2θ fluctuating from 15^0 to 30^0. Sausa et al [152] noticed that the x-ray diffraction results of mesoporous silica Nanoparticles and concluded that there is no reflection at higher angles for mesoporous silica nanoparticles. This indicates that mesoporous silica nanoparticles are not crystalline at the atomic level.

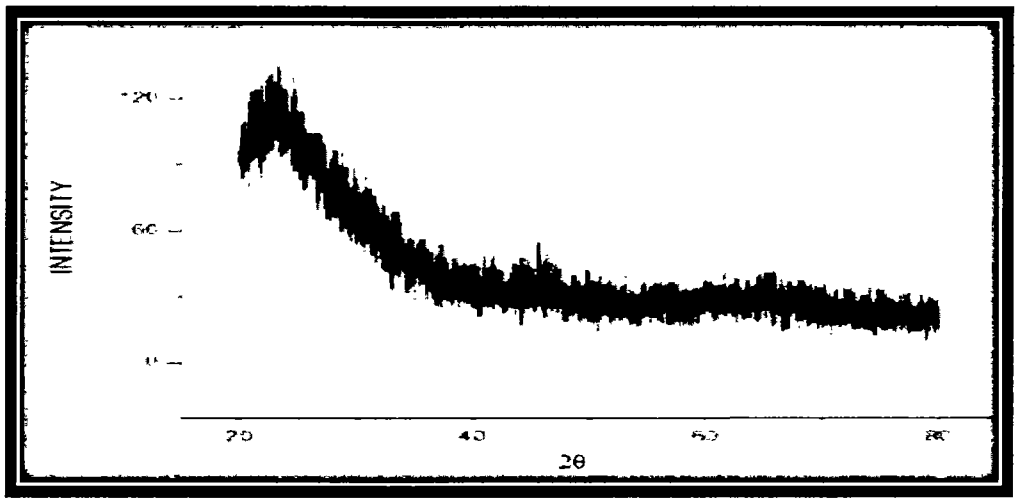

Figure 4.3: XRD pattern of mesoporous silica nanoparticles through hydrothermal method

By comparing the results of mesoporous silica nanoparticles prepared greener route (figure 4.2) and from the hydrothermal method (figure 4.3) is almost identical. The results reveal that the plant which has chemical reducing agent can also be synthesized amorphous silica Nanoparticles.

4.1.3 XRD analysis of Cobalt Ferrite coated on mesoporous silica:

The XRD pattern for cobalt ferrite coated Silica nanoparticles is shown in Figure 4.4. The prominent peaks existent in this figure is those of cobalt ferrite as talk about above. The wide peak at low angles may specify the occurrence of the amorphous Silica. By comparing the result with the JCPDS database for silica and cobalt ferrite shows that the peak at angle $2\theta=35^0$ and $2\theta \approx 37^0$ have a touch of cobalt ferrite. Both of these peaks are vastly concealed by the cobalt ferrite peaks. The result got by Hu et al. [153] and David et al. [146] are close to our measurement.

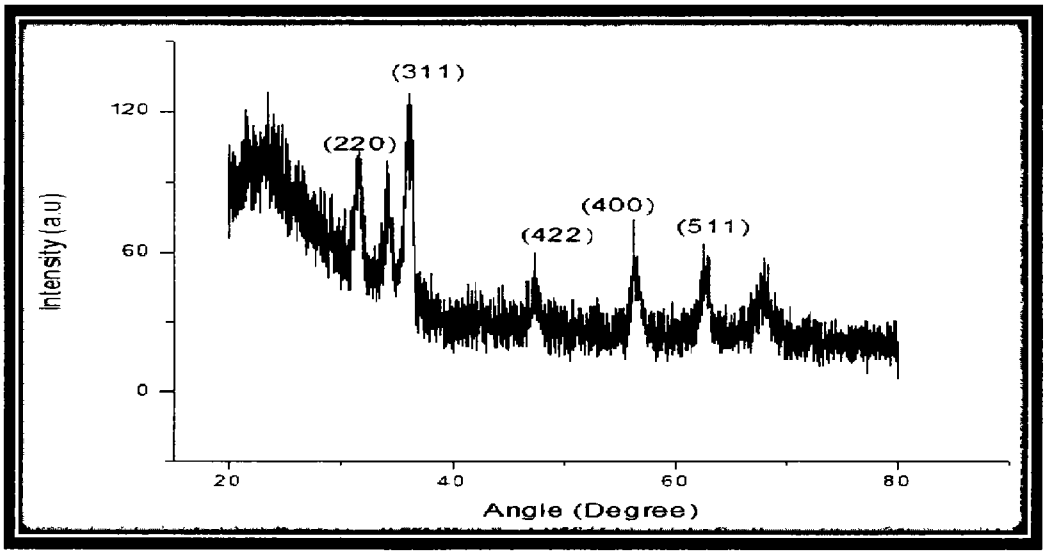

Figure 4.4: XRD pattern of cobalt ferrite coated on mesoporous silica nanoparticles

4.2 Morphological investigation:

4.2.1 Scanning Electron Microscopy (SEM):

4.2.1.1 SEM analysis of Cobalt ferrite Nano particles prepared from greener route:

The SEM images of pure $CoFe_2O_4$ is shown in figure 4.5. This shows that it has agglomeration between the particles, which are relates to the magnetization of ferrites.

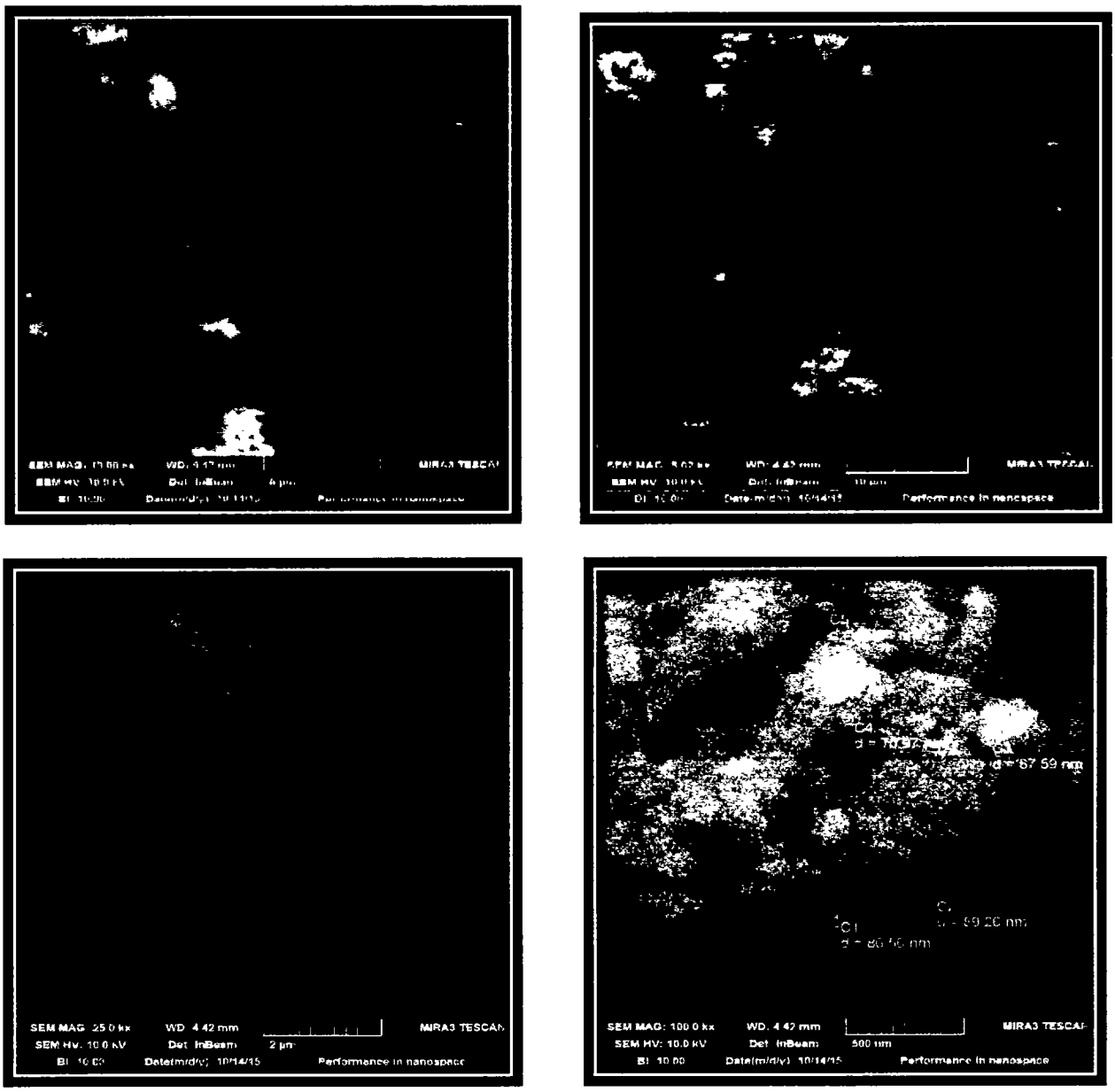

Figure 4.5: SEM images of Cobalt ferrite Nano particles at different resolutions

4.2.1.2 SEM analysis of Mesoporous silica nanoparticles:

Figure 4.6 shows the SEM images of the green synthesized silica nanoparticles. The figures display that the morphology of synthesized nanoparticles of mesoporous silica is spherical. These nanoparticles are 200 nm in size. The SEM images showed that the spherical nanoparticles formed are randomly distributed and agglomerated. Chitra and Annadurai [147] also synthesized spherical randomly distributed agglomerated silica nanoparticles having a size range of 151 – 165 nm by treating with chemical method [154]. The images are revealing that we can use a non-toxic green chemistry procedure for the formation of mesoporous silica nanoparticles deprived of any chemical as a reducing agent. The eco – friendly Neem plant extract represented as the same way a chemical reducing agent represents. In this experimental procedure, we used the phytochemicals that are present in Neem plant extract it powerfully reduced the silica precursor into relevant nanoparticles.

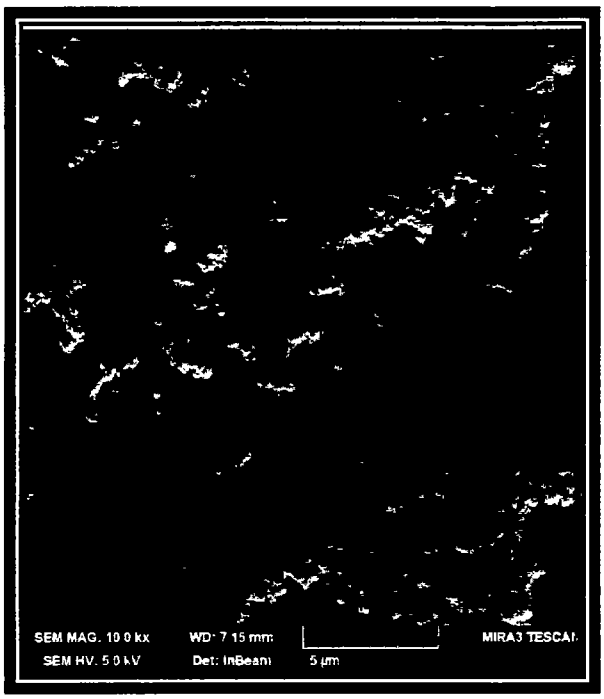

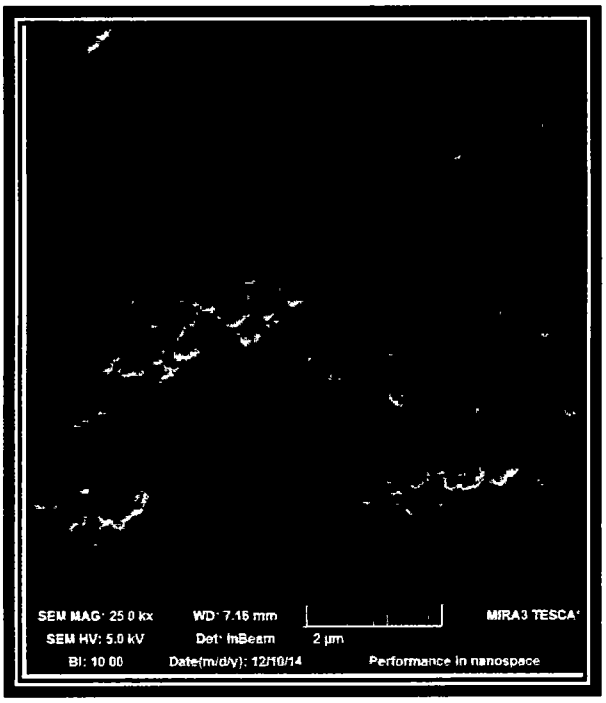

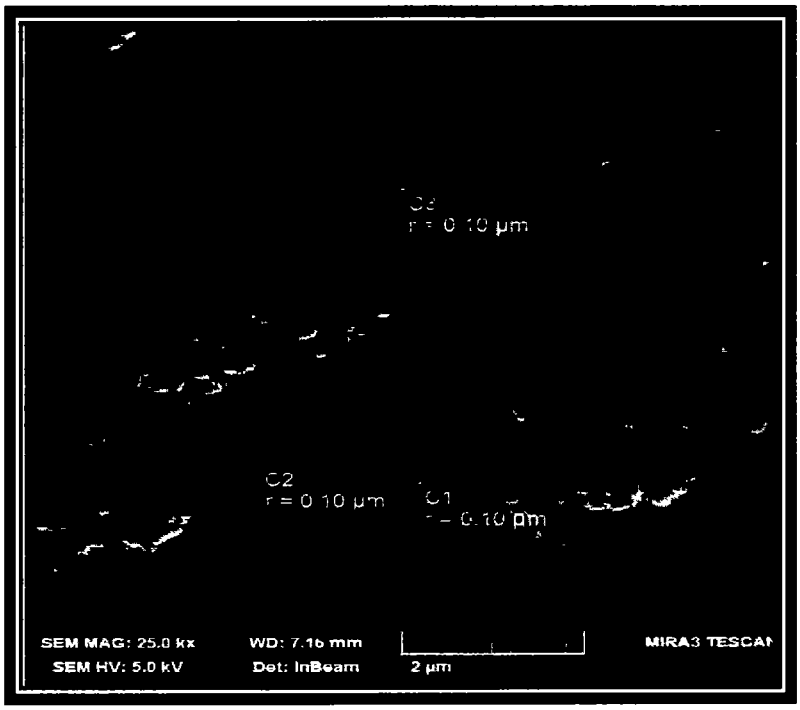

Figure 4.6: SEM image of mesoporous silica through Greener Route at different resolutions

Figure 4.7 shows the SEM result of mesoporous silica nanoparticles prepared by the hydrothermal method. The SEM images show the morphology of nanoparticles is Nanospheres with diameter of 4.5 µm. The average particle diameter is around 87 nm that is suitable for the drug delivery applications. Yan-Tao Shi at .el [155] also synthesized mesoporous silica Nanospheres.

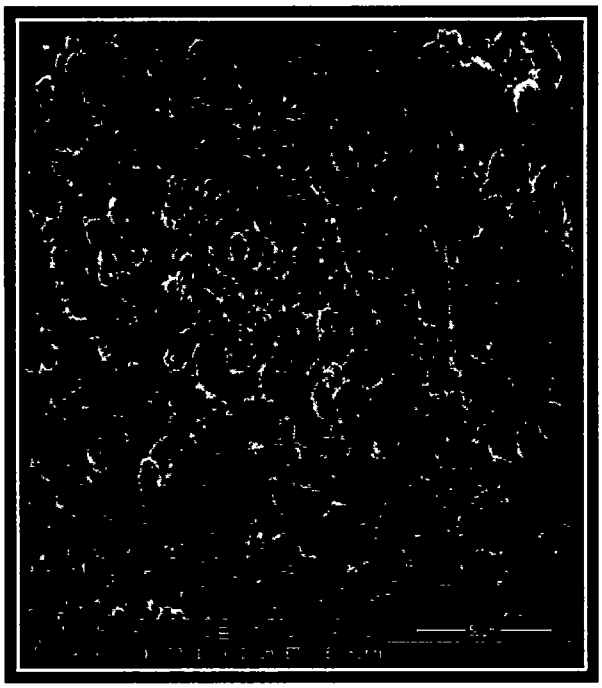

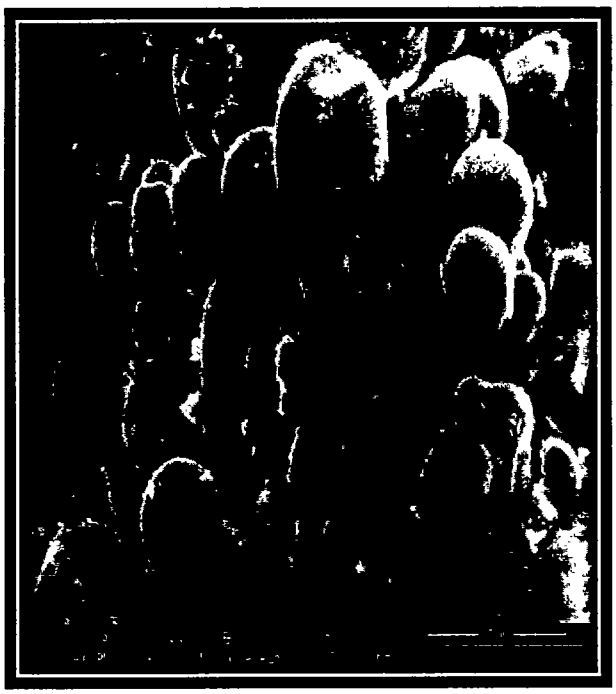

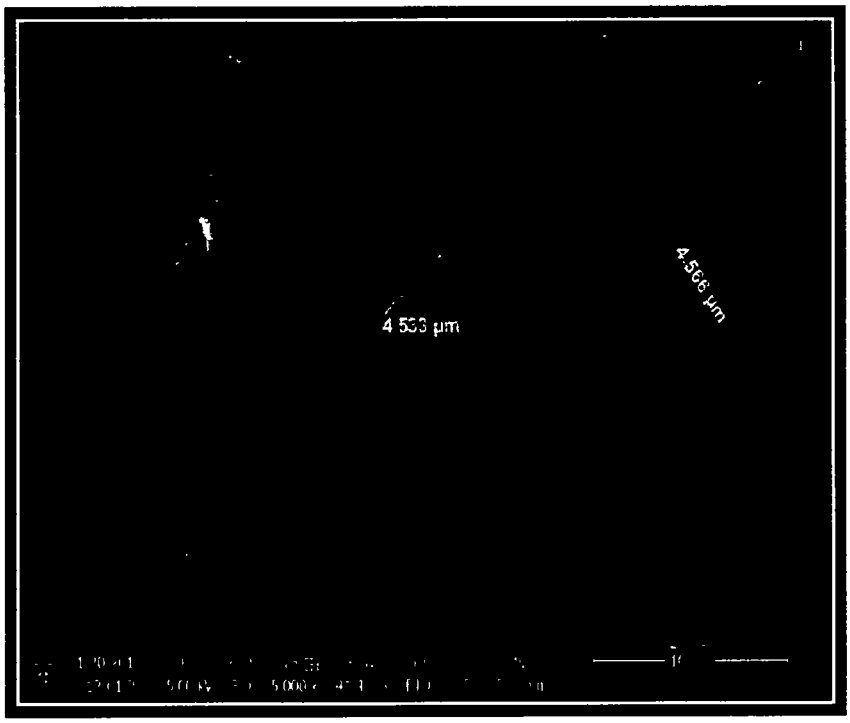

Figure 4.7: SEM image of mesoporous silica through hydrothermal Route at different resolutions

4.2.1.3 SEM analysis of Cobalt Ferrite coated on mesoporous silica:

The SEM images of Cobalt ferrite coated on mesoporous silica nanoparticles are shown in Figure 4.8 and 4.9 particularly show narrow grain size distribution and present mainly sphericity. It can be obviously seen that a cobalt ferrite is enwrapped on the silica surface forming a core-shell structure of Nanocomposites. Figure 4.8 shows the cobalt ferrite coated on mesoporous silica that is synthesized through greener route.

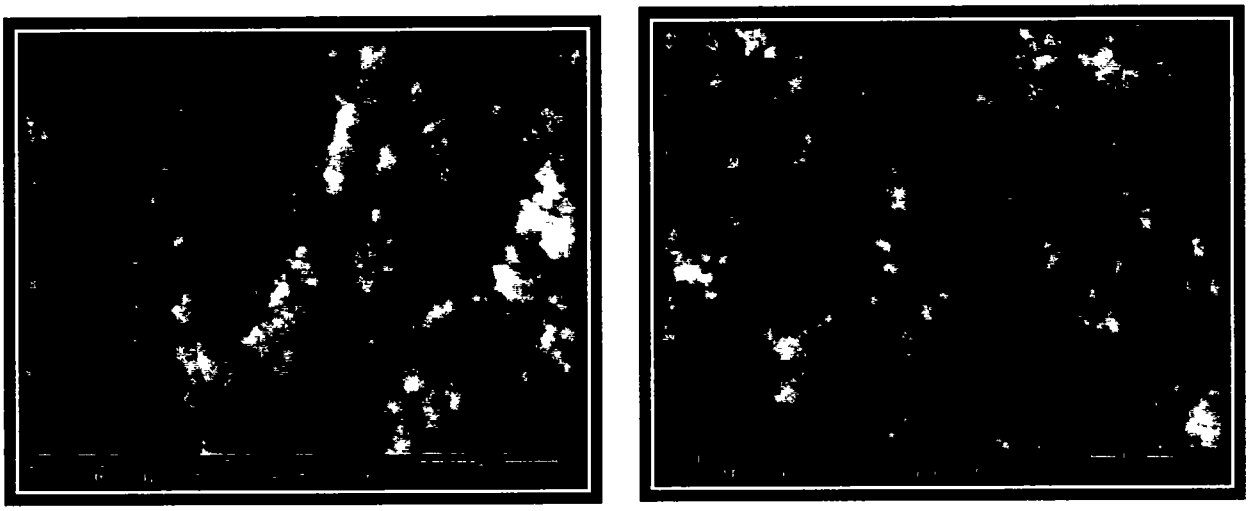

Figure 4.8: SEM images of coblat ferrite coated on mesoporous silica (Greener route) at different resolution

Figure 4.9 shows that cobalt ferrite is coated on mesoporous silica nanosphere, which is synthesized by hydrothermal method with average diameter 8.3 μm.It is clearly seen that due to coating of cobalt ferrite the particle size is increased.

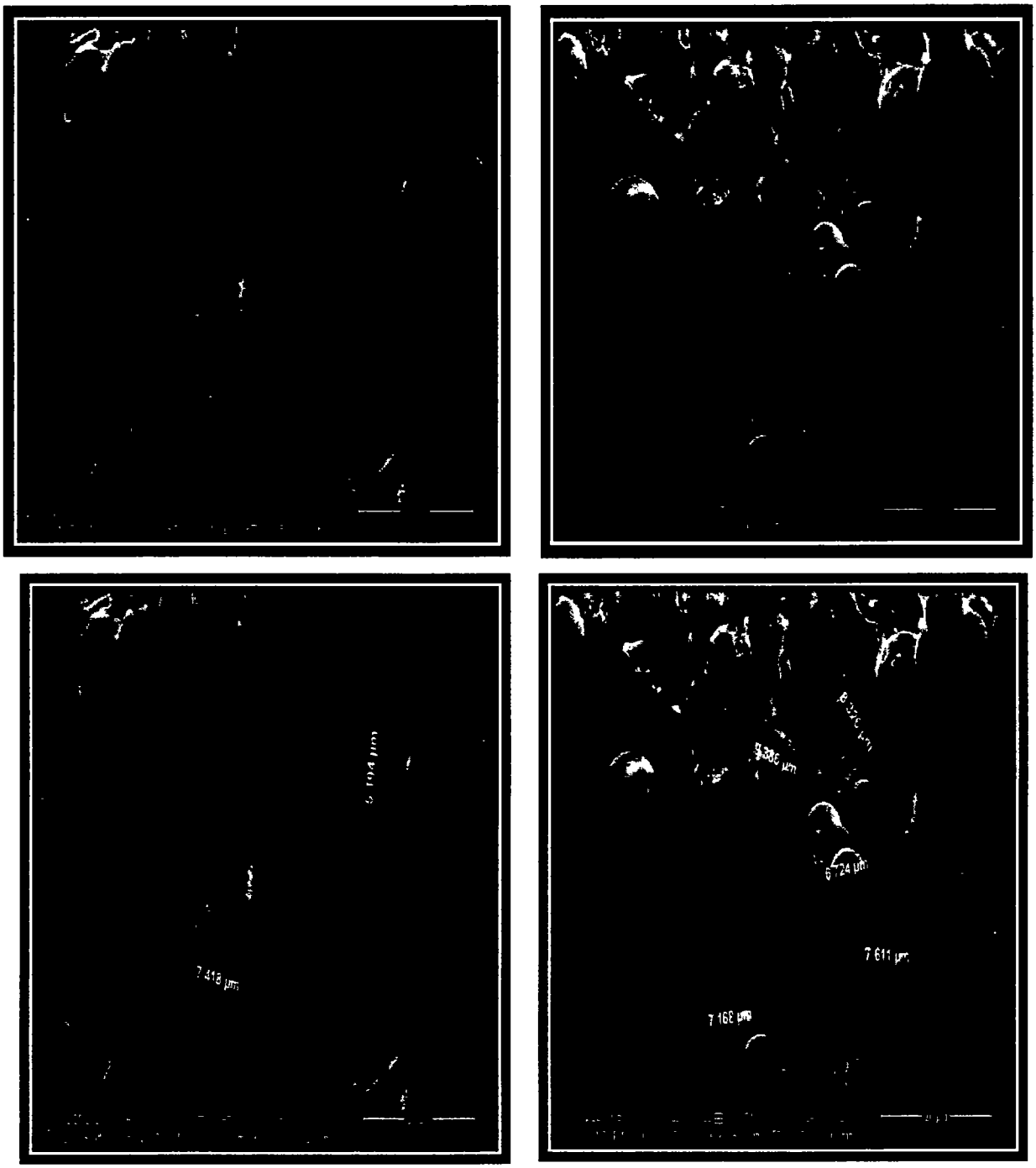

Figure 4.9: SEM images of cobalt ferrite coated on mesoporous silica (hydrothermal route) at different resolutions

4.3 Chemical investigation:

4.3.1 Energy Dispersive X-Ray analysis (EDX):

4.3.1.1 EDX analysis of Cobalt ferrite Nano particles prepared from greener route:

The EDX spectrum of cobalt ferrite is shown in figure 4.10. This spectrum shows the peaks of cobalt, iron and oxygen. This confirms the formation of cobalt ferrite.

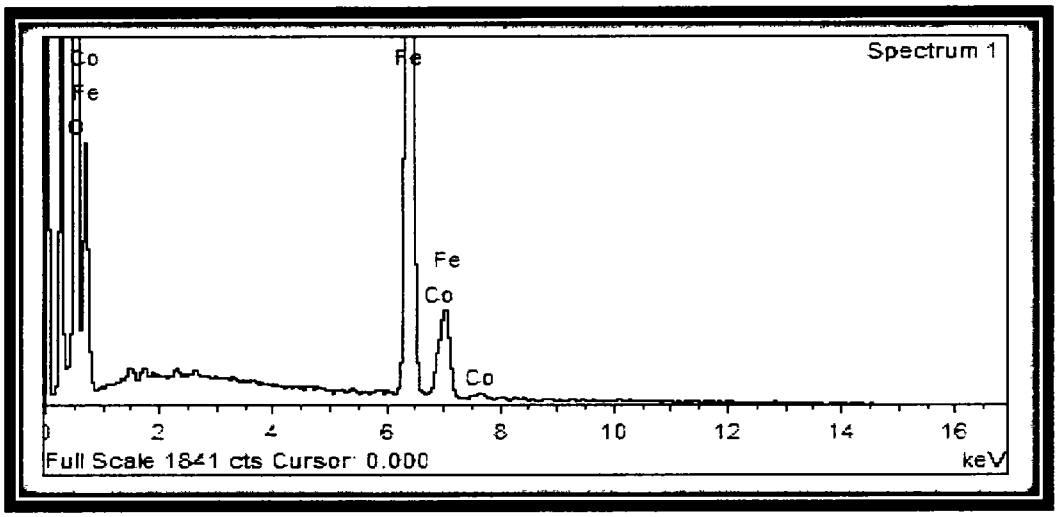

Figure 4.10: EDX spectra of cobalt ferrite

The quantity of cobalt, iron and oxygen in our sample is shown in Table 4.1

Elements	Weight %	Atomic %
O K	38.89	69.04
Fe K	56.37	28.67
Co K	4.74	2.29
Total	100.00	

4.3.1.2 EDX analysis of Mesoporous silica nanoparticles prepared from greener route:

Figure 4.11 indicates the EDX spectrum of silica nanoparticles that are synthesized through greener route. The EDX results sanction the occurrence of element silica. The EDX spectrum also shows the existence of oxygen. The green synthesized silica nanoparticles display optical absorption band peak at 1.8 keV. Chitra and Annadurai [147] also described the silica peak at 1.8 keV and occurrence of carbon and oxygen in the EDX spectrum [154]. There is not much

difference in results for particles synthesized with greener route and through hydrothermal method.

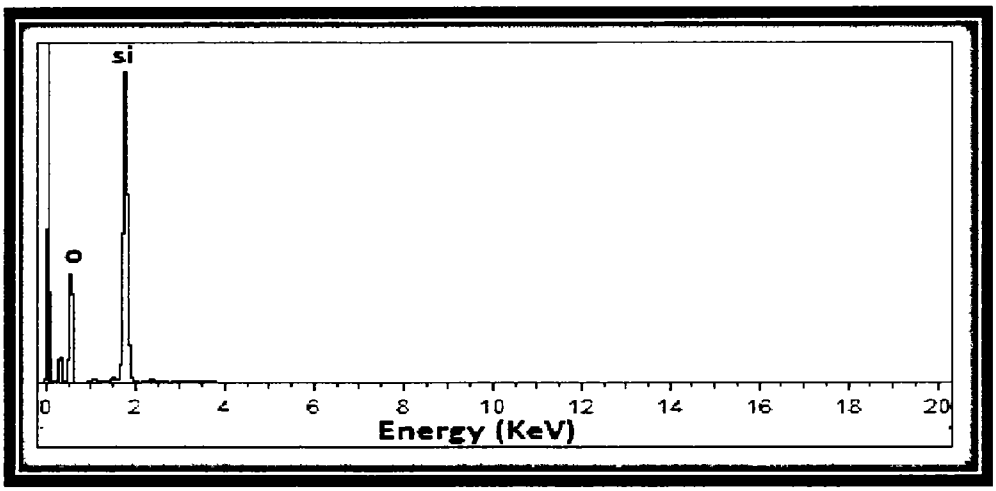

Figure 4.11: EDX spectra of mesoporous silica from greener route

The Chemical composition analysis of silica prepared from greener route.The quantity of silicon and oxygen in our sample is shown in Table 4.2.

Elements	Weight %	Atomic %
O K	36.37	67.04
Si K	63.37	23.67
Total	100.00	

4.3.1.3 EDX analysis of Mesoporous silica nanoparticles prepared from Hydrothermal Method:

The EDX spectrum of silica that is prepared from hydrothermal route is shown in figure 4.12. This spectrum shows the peaks of silicon and oxygen. This confirms the formation of silica.

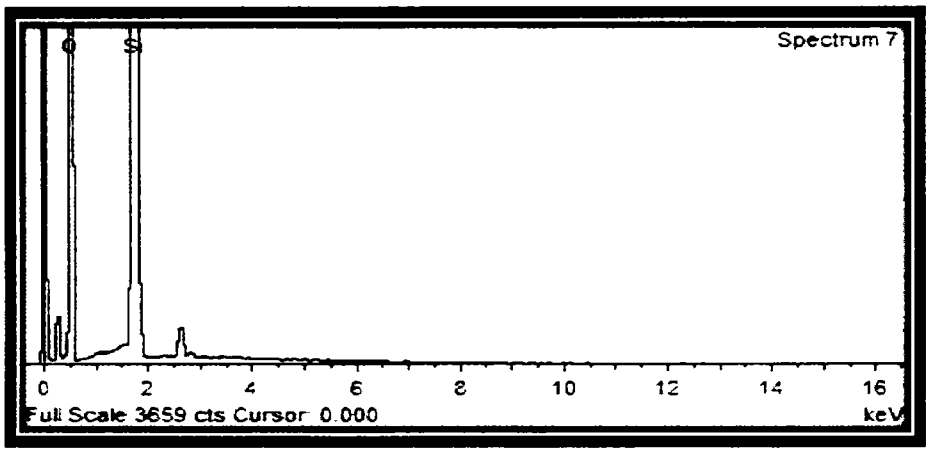

Figure 4.12: EDX spectra of mesoporous silica through hydrothermal method

The chemical composition analysis of silica through hydrothermal method is shown in table 4.3. The quantity of silicon and oxygen in our sample are:

Elements	Weight %	Atomic %
O K	57.02	69.96
Si K	42.98	30.04
Total	100.00	

4.3.1.4 EDX analysis of Cobalt Ferrite coated on mesoporous silica:

The EDX spectrum of silica is shown in figure 4.13. This spectrum shows the peaks of silicon, oxygen and iron. This shows the elemental composition of cobalt ferrite.

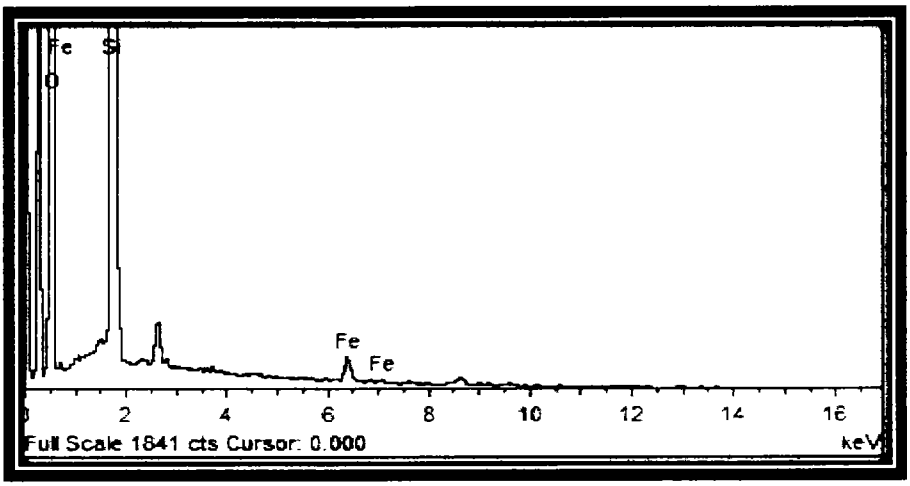

Figure 4.13: EDX spectra of cobalt ferrite coated on mesporous silica

The chemical composition analysis of cobalt ferrite coated on mesporous silica is shown in table 4.4 The quantity of silicon, oxygen and iron in our sample are:

Elements	Weight %	Atomic %
O K	62.13	72.24
Fe K	2.17	0.75
Si K	34.13	23.54
Total	100.00	

4.4 Optical studies:

4.4.1 UV-Visible absorption spectroscopy:

4.4.1.1 UV-Visible analysis of Cobalt ferrite Nano particles prepared from greener route:

The spectrum of UV-Visible spectroscopy of cobalt ferrite is shown in figure 4.14.It shows Maximum absorbance peak is at 260 nm and have Band gap 3.3 eV.

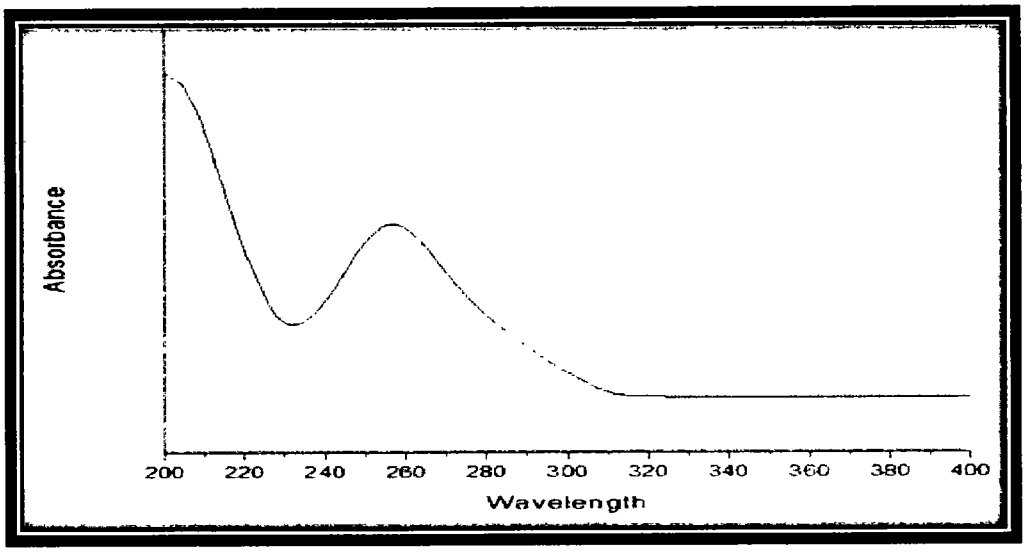

Figure 4.14: UV-Visible analysis of Cobalt ferrite Nano particles prepared from greener route

4.4.1.2 UV-Visible analysis of Mesoporous silica nanoparticles:

The spectrum of UV-Visible spectroscopy of mesoporous silica prepare from greener route is shown in figure 4.13. It shows Maximum absorbance peak is at 260 nm and have Band gap 4.1 eV.

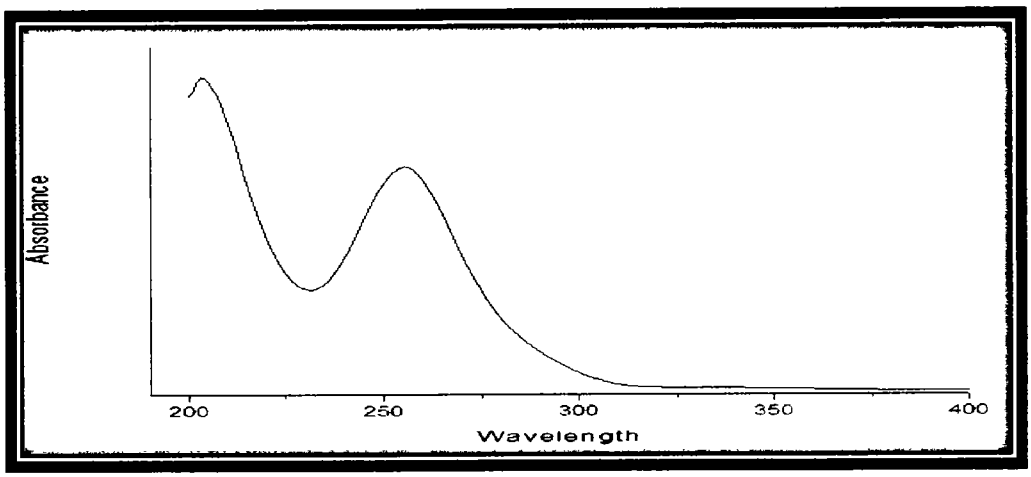

Figure 4.15: UV-Visible analysis of Mesoporous silica nanoparticles prepared from greener route

The spectrum of UV-Visible spectroscopy of mesoporous silica nanoparticles prepared from hydrothermal method is shown in figure 4.16. It shows Maximum absorbance peak is at 270 nm and have Band gap 3.4 eV.

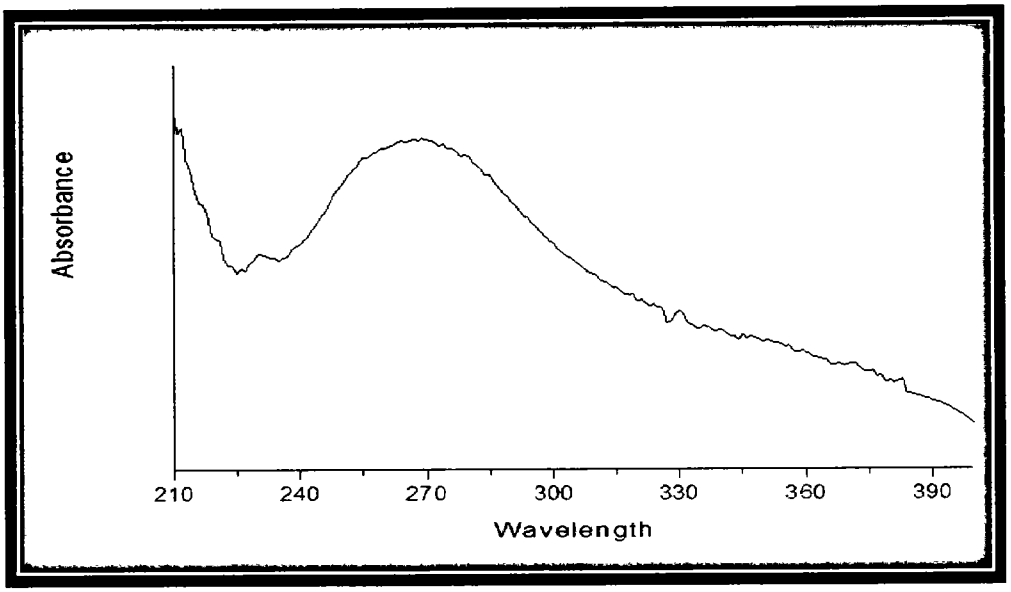

Figure 4.16: UV-Visible spectrum of Mesoporous silica nanoparticles prepared from Hydrothermal Method

4.4.1.3 UV-Visible analysis of Cobalt Ferrite coated on mesoporous silica:

The spectrum of UV-Visible spectroscopy of cobalt ferrite coated on mesoporous silica nanoparticles is shown in figure 4.15. It shows Maximum absorbance peak is at 250 nm and have Band gap 4.1 eV.

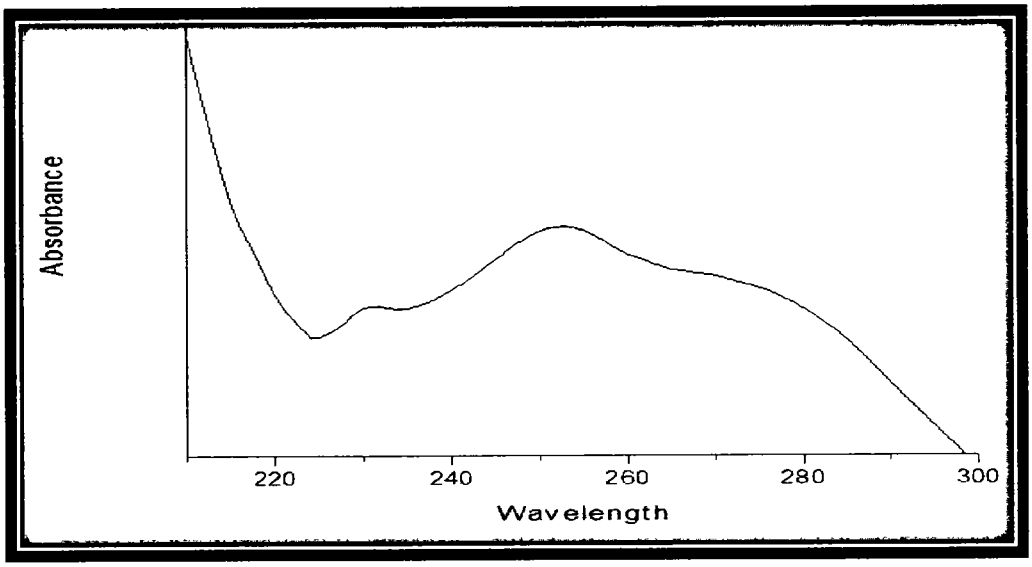

Figure 4.17: UV-Visible analysis of Cobalt Ferrite coated on mesoporous silica

4.5 Drug loaded pattren:

4.5.1 Fouier transform infra-red spectroscopy(FTIR):

4.5.1.1 FTIR analysis of Cobalt ferrite Nano particles prepared from greener route:

The FTIR spectra were noted on FTIR spectrophotometer using the KBr pellet method. FTIR spectra of cobalt ferrite is represented in figure 4.18(a). From the FTIR spectra it is seen that there are absorbance peaks at lower frequency at about 700 to 510 cm^{-} .it can be attributed to the stretching vibration of the Metal-oxygen (M-O) in tetrahedral and octahedral sites respectively. This can be endorsed to the high degree of crystalline feature of cobalt ferrite nanostructures. The small bands 1620 and 1390 cm^{-1} are assigned to the asymmetric symmetric stretching of COO groups.

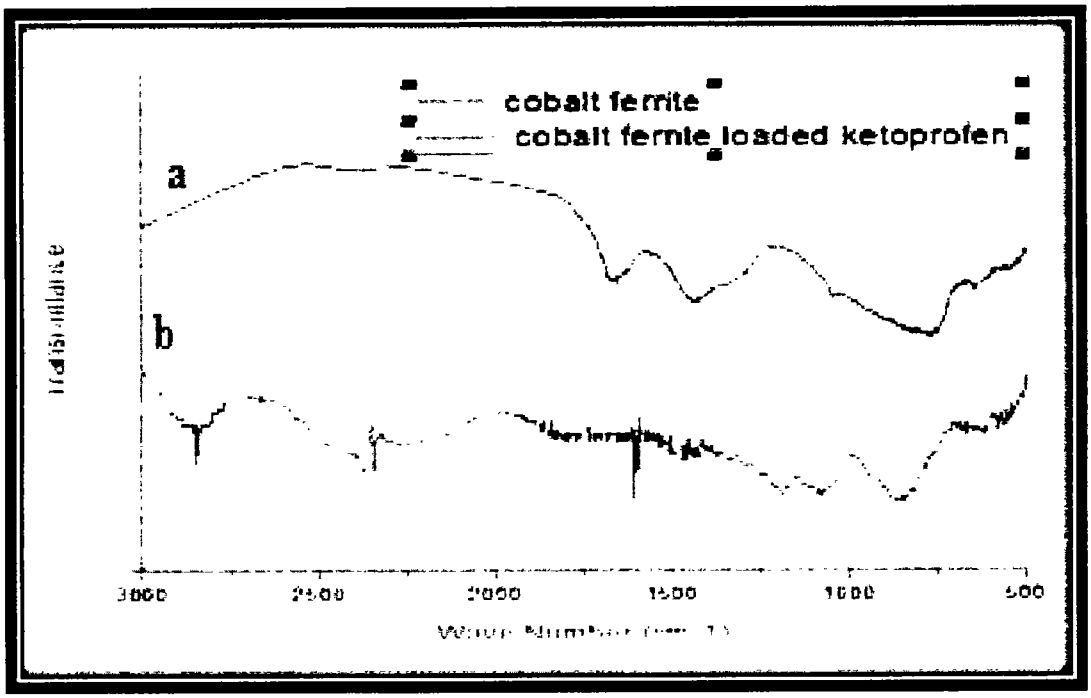

Figure 4.17: FTIR spectra of cobalt ferrite nanoparticles (a) cobalt ferrite nanoparticles (b) cobalt ferrite nanoparticles loaded with Ketoprofen

In figure 4.17 (b) there is drug loaded peaks of cobalt ferrite nanostructures. In this spectra of Ketoprofen loaded cobalt ferrite shows weak peak at 2983-2970 cm^{-1} due to the occurrence of an Aromatic C-H stretch carboxylic acid O-H stretch where as at 1450- 1560 cm^{-1} due to the existence

of C=O stretch, at 1590 cm^{-1} Aromatic C=C stretch, at 1437 cm^{-1} due to incidence of $CH-CH_3$ deformation, at 2892 cm^{-1} due to the presence of C-H stretch plus O-H deformation, and at 860-640 cm^{-1} due to existence of C-H out of plane deformation for substituted aromatic.

4.5.1.2 FTIR analysis of Mesoporous silica nanoparticles:

The FTIR spectra of mesoporous silica Nano spheres prepared by chemical route is represented in figure 4.18. in figure 4.18 (a) the absorbance band at 800 cm-1is due to Si-O bond .the strongest IR absorption band is at 1550 cm-1 shows the presence of Si-O-Si bonding whereas absorption band at 990 cm^{-1} and 1100 cm^{-1} also shows Si-O-Si bonding. The absorption band at 1750 cm^{-1} is due to presence of OH group.

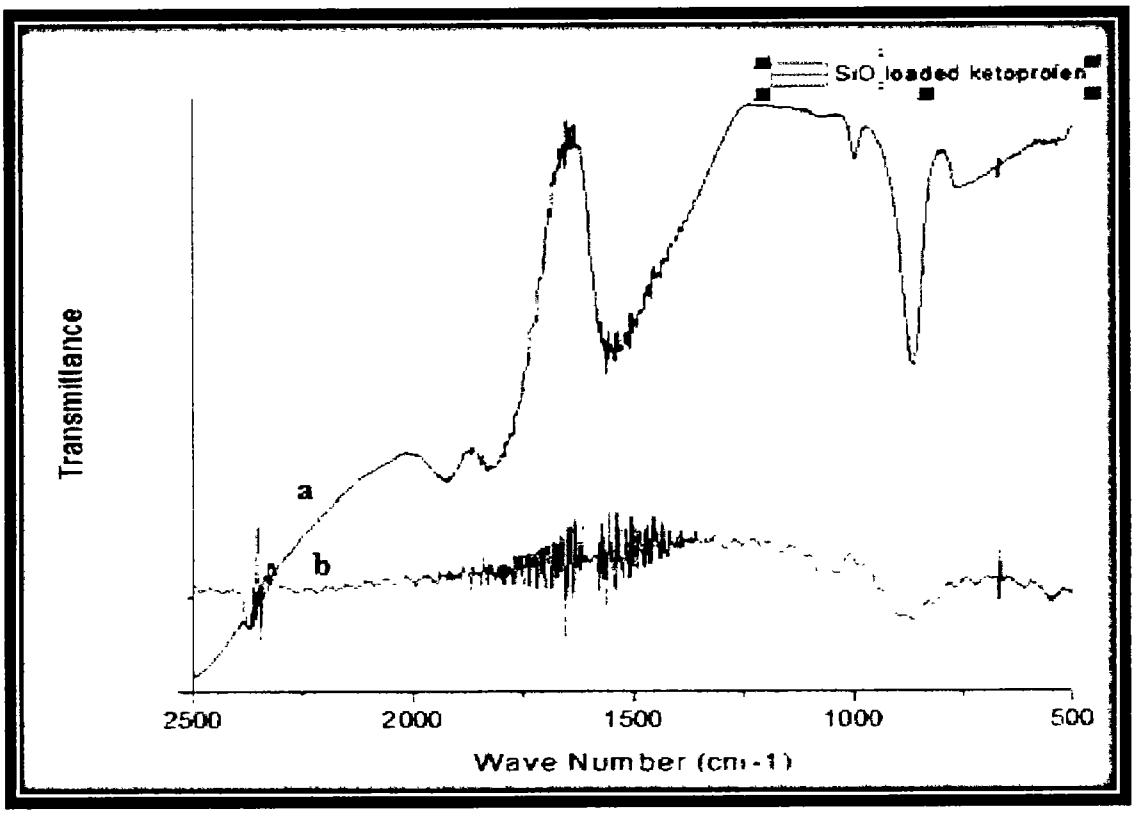

Figure 4.18: FTIR spectra of mesoporous silica nanoparticles (hydrothermal route) (a) mesoporous silica nanoparticles (b) mesoporous silica nanoparticles loaded with Ketoprofen

In figure 4.18 (b) IR peaks of silica loaded with Ketoprofen is shown. In this spectra of Ketoprofen loaded mesoporous silica (chemical) shows peak of C=O stretch at 1350- 1560 cm^{-1}, Aromatic

C=C stretch at 1690 cm^{-1}, and a peak at 860 cm^{-1} due to existence of C-H out of plane deformation for substituted aromatic.

The FTIR spectra of mesoporous silica Nano spheres prepared by greener route is represented in figure 4.19. in figure 4.19 (a) the absorbance band at 750 cm^{-1} is due to Si-O bond .The IR absorption band is at 1470 cm^{-1} shows the presence of Si-O-Si bonding whereas absorption band at 1050 cm^{-1} also shows Si-O-Si bonding. The absorption band at 1750 and 2300 cm^{-1} is due to presence of OH group.

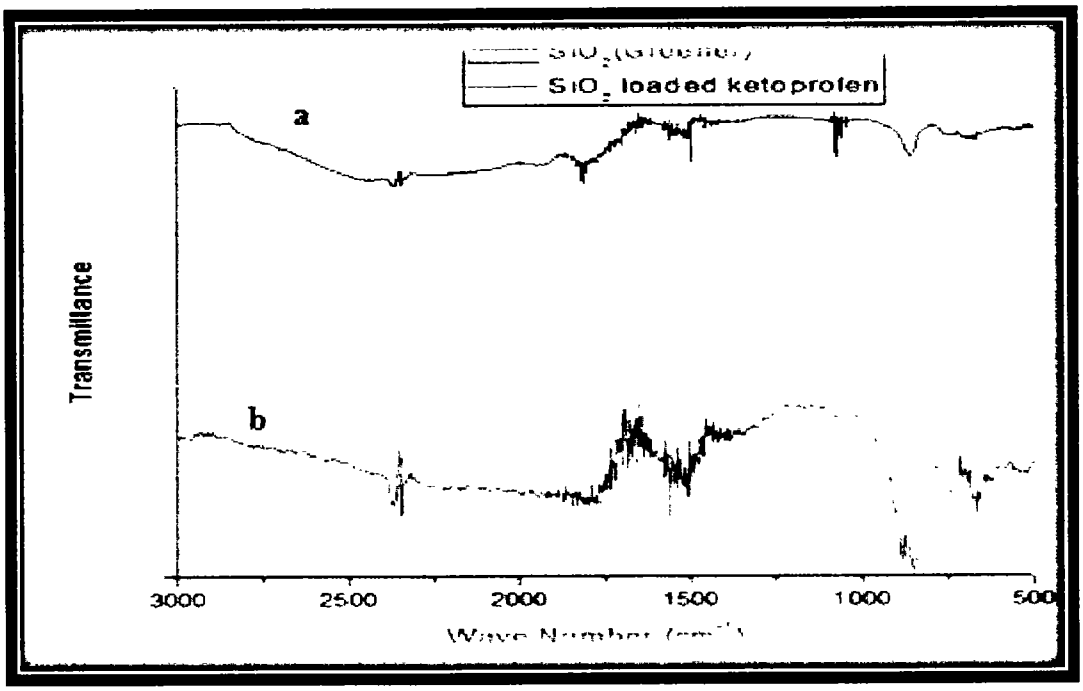

Figure 4.19: FTIR spectra of mesoporous silica nanoparticles (greener route) (a) mesoporous silica nanoparticles (b) mesoporous silica nanoparticles loaded with Ketoprofen

In figure 4.19 (b) IR peaks of mesoporous silica (greener route) loaded with Ketoprofen is shown. In this spectra of Ketoprofen loaded mesoporous silica (chemical) shows peak of C=O stretch at 1450- 1530 cm^{-1}, Aromatic C=C stretch at 1730 cm^{-1}, at 1420 cm^{-1} due to incidence of $CH\text{-}CH_3$ deformation and a peak at 860-650 cm^{-1} due to existence of C-H out of plane deformation for substituted aromatic.

4.5.1.3 FTIR analysis of Cobalt Ferrite coated on mesoporous silica:

The FTIR spectra were noted on FTIR spectrophotometer using the KBr pellet method. FTIR spectra of cobalt ferrite coated on mesoporous silica is represented in figure 4.20 (a). From the

FTIR spectra it is seen that there are absorbance peaks at about 700 to 510 cm^{-1}.is of cobalt ferrite. The silica peaks can be seen at 800, 1100, 1750 and 2300 cm^{-1}.

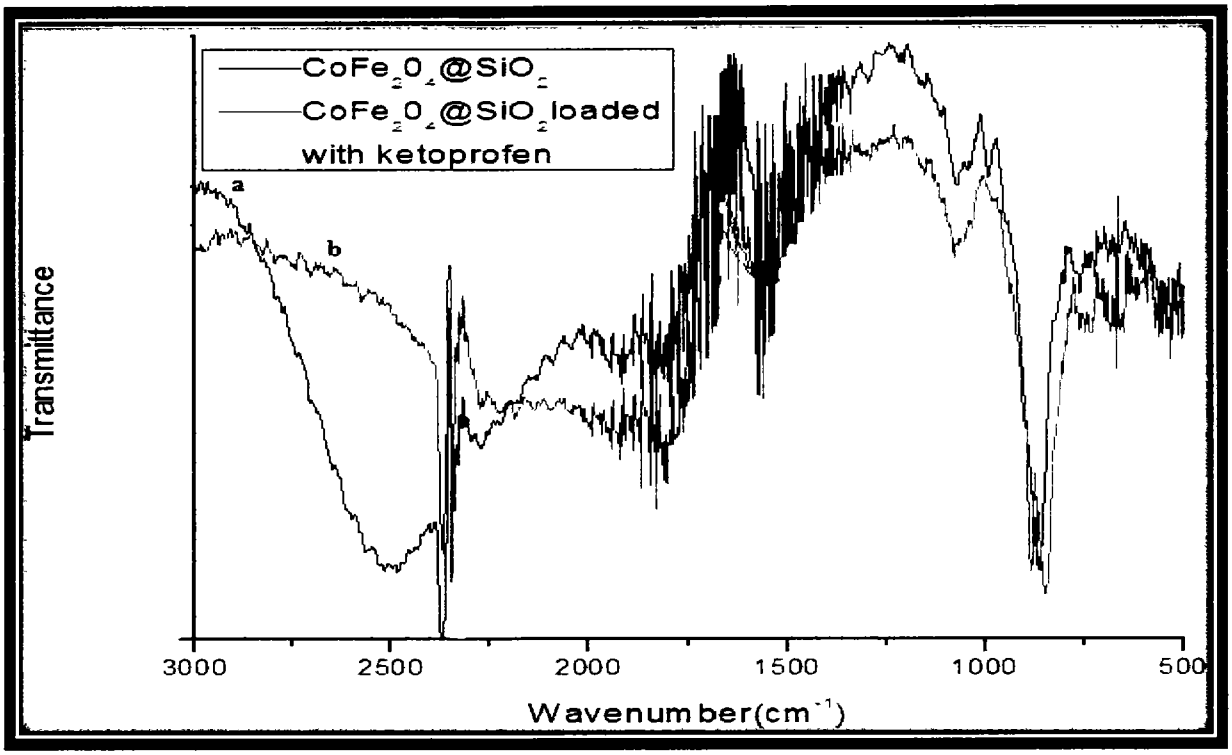

Figure 4.20: FTIR spectra of Cobalt Ferrite coated on mesoporous silica nanoparticles (a) Cobalt Ferrite coated on mesoporous silica nanoparticles (b) Cobalt Ferrite coated on mesoporous silica nanoparticles loaded with Ketoprofen

In figure 4.20 (b) IR peaks of cobalt ferrite coated on mesoporous silica loaded with Ketoprofen is shown. The peak of C=O stretch at 1450- 1530 cm^{-1}, Aromatic C=C stretch at 1730 cm^{-1}, at 1420 cm^{-1} due to incidence of CH-CH_3 deformation and a peak at 860-720 cm^{-1} due to existence of C-H out of plane deformation for substituted aromatic.

4.6 Drug release pattren:

Figure 4.21 shows the drug Ketoprofen releasing pattern from cobalt ferrite, mesporous silica and their composites. The release was checked in PBS buffer with pH value 7.4 at 37°.the pH value of 7.4 mimic the physiological pH of blood.

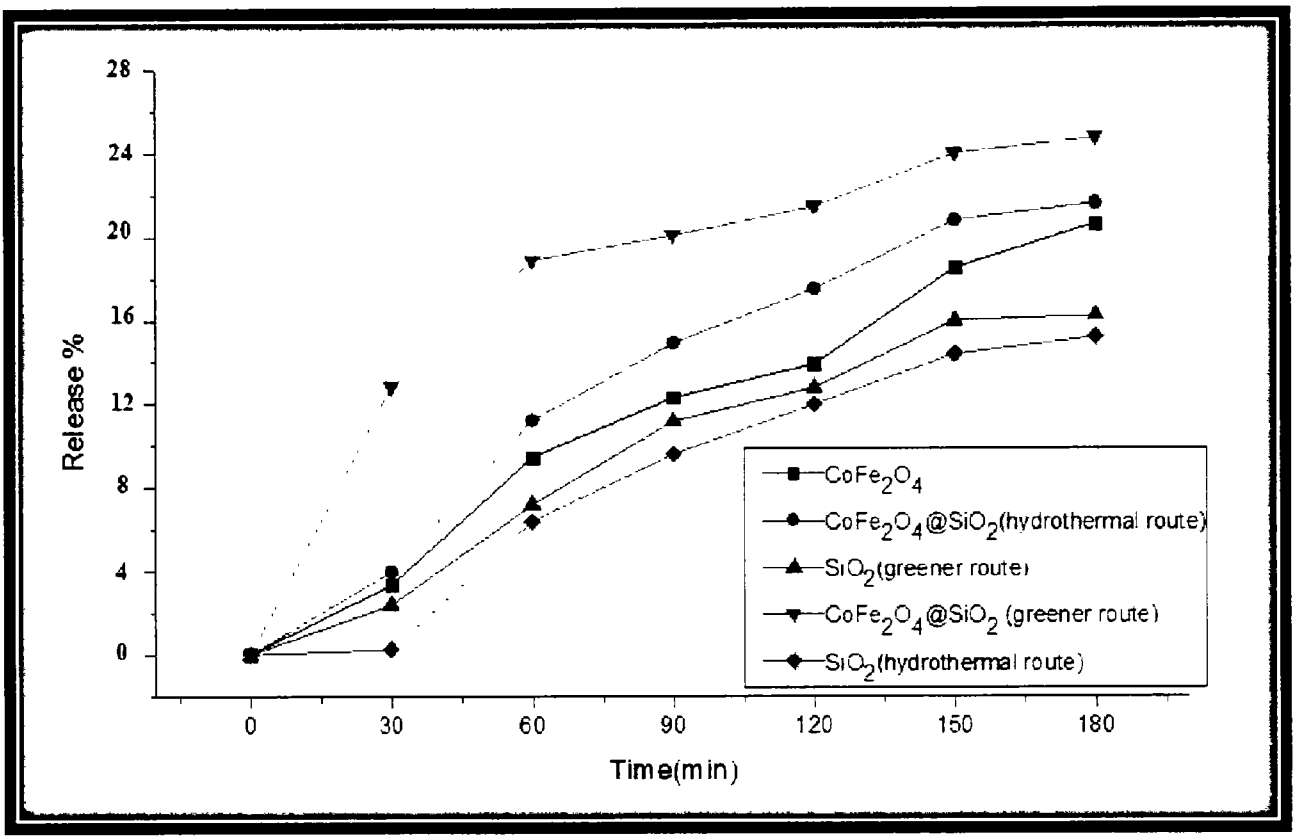

Figure 4.21: Drug ketoprofen releasing pattren

The drug release pattern shows a continues release till 60 min with a maximum of 20% absorbed drug released from the cobalt ferrite coated on mesoporous silica nanoparticles that is prepared by greener route and 11.5% maximum release from cobalt coated on mesoporous silica particles that is prepared from hydrothermal route in 60 min. At time 60 min the maximum release of absorbed drug is 10.5 % from cobalt ferrite, 7.5% from mesoporous silica that is prepared from greener route and 7% from mesoporous silica prepared from hydrothermal route. These results shows that green synthesized silica nanoparticles and its nanocomposite potentially work as vehicle for drug delivery applications with benefit of biocompatibility and non –toxic protective surface.

Conclusions

The different route has been adopted for the synthesis of pure-silica, cobalt ferrite, and their Nanocomposites. Then the samples were compared by using different characterization tools like XRD, SEM, EDX, FTIR and UV-Visible spectroscopy. Due to the coating of cobalt ferrite, it increases the magnetic nature of silica. XRD shows that mesoporous silica is amorphous substance. SEM results indicate the formation of mesoporous silica Nanospheres. By comparing SEM results of hydrothermal route and greener route it is found that through greener route we obtained Nanospheres whereas from the hydrothermal route we got microspheres. EDX analysis confirms the formation of silica and cobalt ferrite. It was found that both results are comparable but green synthesis provides us an eco-friendly way for the synthesis of nanomaterials. The use of plant extract for the synthesis of nanomaterials is also economical. FTIR spectra show the successful loading of Ketoprofen on silica and cobalt ferrite and their nanocomposites. From the drug release pattern, we concluded that nanocomposite that is prepared from greener route gives good results as compared to nanocomposite that is prepared from the hydrothermal method. It is determined that it shows good results in drug delivery applications. Magnetic Nanoparticles may soon play a significant role in meeting the healthcare needs of tomorrow.

REFERENCES

1. P. Poizot, S.L., S. Grugeon, L. Dupont, J.M. Tarascon, Nano-sized transitionmetaloxides as negative-electrode materials for lithium-ion batteries. Natue, 2000. **407** (6803): p. 496–499.
2. A. Tari, R.W.C., S.W. Charles, J. Popplewell, Magnetic-properties and stability of a ferrofluid containing Fe_3O_4 particles. Physica B & C, 1979. **97**(1): p. 57–64.
3. M. Mahmoudi, A.S., M. Imani, P. Stroeve, A. Sohrabi, Templated growth of superparamagnetic iron oxide nanoparticles by temperature programming in the presence of poly(vinyl alcohol). Thin Solid Films, 2010. **518**(15): p. 4281–4289.
4. Morteza Mahmoudi, S.S., Ben Wang, Sophie Laurent, Tapas Sen, Super paramagnetic iron oxide nanoparticles (SPIONs): Development, surface modification and applications in chemotherapy. Advanced Drug Delivery Reviews 2011. **63**: p. 24–46.
5. D. Peer, J.M.K., S. Hong, O.C. Farokhzad, R. Margalit, R. Langer Nanocarriers as an emerging platform for cancer therapy. Nat. Nanotechnol, 2007. **2**: p. 751—760.
6. R.K. Jain, T.S., Delivering nanomedicine to solid tumors. Nat. Rev. Clin. Oncol., 2010. **7**: p. 653—664.
7. R.A. Petros, J.M.D., Strategies in the design of nanoparticles for therapeutic applications. Nat. Rev. Drug Discov, 2010. **9**: p. 615—627.
8. Duncan, R., Polymer conjugates as anticancer nanomedicines. Nat. Rev. Cancer 2006. **6**: p. 688—701.
9. M.E. Davis, Z.C., D.M. Shin, Nanoparticle therapeutics: an emerging treatment modality for cancer. Nat. Rev. Drug Discov., 2008. **7**: p. 771—782.
10. Ferrari, M., Cancer nanotechnology: opportunities and challenges. Nat. Rev. Cancer, 2005. **5**: p. 161—171.
11. L. Zhang, F.X.G., J.M. Chan, A.Z. Wang, R.S. Langer, O.C. Farokhzad, Nanoparticles in Medicine: Therapeutic Applications and Developments. Clin. Pharmacol. Ther, 2008. **83**: p. 761-769.
12. B.Y.S. Kim, J.T.R., W.C.W. Chan, Nanomedicine. N. Engl. J. Med. , 2010. **363**: p. 2434—2443.
13. Dahl JA, M.B., Hutchison Toward Greener Nanosynthesis. JE. Chem Rev 2007. **107**: p. 2228–2269.
14. Hutchison, Selective Growth of Vertical ZnO Nanowire Arrays Using Chemically Anchored Gold Nanoparticles. JE. ACSNano 2008. **2**(10): p. 2001–2006.
15. Karn, B., The Road to Green Nanotechnology. 2008. **12**(3): p. 263–266.
16. Debjani Nath, P.B., Green nanotechnology – A new hope for medical biology. Environmental Toxicology and Pharmacology, 2013. **36**(3): p. 997–1014.
17. Kirchhoff, P.T.A.a.M.M., Origins, Current Status, and Future Challenges of Green Chemistry. Acc. Chem. Res., 2002. **35**(9): p. 686–694.
18. Anstas PT, W.J., Green Chemistry: Principles and Practice. Chemical Society Reviews, 2010. **39**: p. 301-312.
19. Martyn Poliakoff, J.M.F., Trevor R. Farren, Paul T. Anastas, Green Chemistry: Science and Politics of Change. Science, 2002. **297**: p. 807-810.
20. Poovathinthodiyil Raveendran , J.F., and Scott L. Wallen, Completely "Green" Synthesis and Stabilization of Metal Nanoparticles. J. Am. Chem. Soc, 2003. **125**(46): p. 13940–13941.

21. Raveendran P, F.J., Wallen SL, A simple and "green" method for the synthesis of Au, Ag, and Au–Ag alloy nanoparticles. Green Chemistry, 2006. **8**: p. 34-38.
22. Kumar, V., Yadav, S.K., Plant-mediated synthesis of silver and gold nanoparticles and their applications. J. Chem. Technol. Biotechnol, 2009. **84**: p. 151–157.
23. Satyavathi, R., Krishna, M.B., Rao, S.V., Saritha, R., Rao, D.N., Biosynthesis of silver nanoparticles using Coriandrum sativum leaf extract and their application in non-linear optics. Adv. Sci. Lett., 2010. **3**: p. 1–6.
24. Bar, H., Bhui, D.K., Sahoo, G.P., Sarkar, P., De, S.P., Misra, Green synthesis of silver nanoparticles using latex of Jatropha curcas. Colloids and Surfaces A: Physicochemical and Engineering Aspects, 2009. **339**: p. 134–139.
25. Jha, A.K., Prasad, K, Green synthesis of silver nanoparticles using Cycas leaf. Int. J. Green Nanotechnol., Phys. Chem., 2010. **1**: p. 110-117.
26. Ali, S.A.Y.a.S., Why Nanoscience and Nanotechnology? What is there for us? Journal of Faculty of Engineering & Technology, 2007-2008: p. 11-20.
27. I.I. Slowing, J.L.V.-E., C.W. Wu, V.S.Y. Lin, Mesoporous silica nanoparticles as controlled release drug delivery and gene transfection carriers. Adv. Drug Deliv. Rev., 2008. **60**: p. 1278—1288.
28. Alexander Liberman, N., WilliamC.Trogler, AndrewC.Kummel, Synthesis and surface functionalization of silica nanoparticles for nanomedicine. Surface Science Reports, 2014. **69**: p. 132–158.
29. M.Vallet-Regi, F.B., D.Arcos, Mesoporous Materials for Drug Delivery. Angew.Chem.Int.Ed, 2007. **46**: p. 7548—7558.
30. C. Barbe, J.B., L.G. Kong, K. Finnie, H.Q. Lin, M. Larkin, S. Calleja, A. Bush, G. Calleja, silica nanoparticles:a nolvel drug delivery system. Adv. Mater, 2004. **16**: p. 1959—1966.
31. Di Renzo, F.T., F.; Chen, J. D.; Cambon, H.; Galarneau, A.; Plee, D.; Fajula, F., Textural control of micelle-templated mesoporous silicates: the effects of co-surfactants and alkalinity. Microporous and Mesoporous Materials 1999. **28**(3): p. 437.
32. Tanev, P.T.P., T. J. , Mesoporous Silica Molecular Sieves Prepared by Ionic and Neutral Surfactant Templating: A Comparison of Physical Properties. Chemistry of Materials 1996. **8**: p. 2068–2079.
33. Cai, Q.L., Z.-S.; Pang, W.-Q.; Fan, Y.-W.; Chen, X.-H.; Cui, F.-Z., Dilute Solution Routes to Various Controllable Morphologies of MCM-41 Silica with a Basic Medium. Chemistry of Materials 2001. **13**: p. 258–263.
34. Davidson, A., Modifying the walls of mesoporous silicas prepared by supramolecular-templating. Current Opinion in Colloid & Interface Science, 2002. **7**: p. 92–106.
35. Lin, H.-P.K., C.-P.; Mou, C.-Y.; Liu, S.-B., Counterion Effect in Acid Synthesis of Mesoporous Silica Materials. The Journal of Physical Chemistry B 2000. **104**: p. 7885–7894.
36. Giraldo, L.F.L., B. L.; Pérez, L.; Urrego, S.; Sierra, L.; Mesa, M., Mesoporous Silica Applications. Macromolecular Symposia 2007. **258**: p. 129–141.
37. Ramírez, A.L., B. L.; Sierra, L., Study of the Acidic Sites and Their Modifications in Mesoporous Silica Synthesized in Acidic Medium under Quiescent Conditions. The Journal of Physical Chemistry B, 2003. **107**: p. 9275–9280.
38. Zhao, X.S.L., G. Q., Modification of MCM-41 by Surface Silylation with Trimethylchlorosilane and Adsorption Study. The Journal of Physical Chemistry B, 1998. **102**: p. 1556–1561.
39. Zhao, X.S.L., G. Q.; Millar, G. , Advances in Mesoporous Molecular Sieve MCM-41. J. Industrial & Engineering Chemistry Research, 1996. **35**: p. 2075–2090.

40. Göltner-Spickermann, C., Non-ionic templating of silica: formation mechanism and structure. Current Opinion in Colloid & Interface Science, 2002. **7**: p. 173–178.
41. Sayari, A.H., S. , Periodic Mesoporous Silica-Based Organic–Inorganic Nanocomposite Materials. Chemistry of Materials, 2001. **13**: p. 3151–3168.
42. Soler-Illia, G.J.d.A.A.C., E. L.; Grosso, D.; Sanchez, C., Block copolymer-templated mesoporous oxides. Current Opinion in Colloid & Interface Science, 2003. **8**: p. 109–126.
43. Grün, M.K., A. A.; Schacht, S.; Schüth, F.; Unger, K. K., Comparison of an ordered mesoporous aluminosilicate, silica, alumina, titania and zirconia in normal-phase high-performance liquid chromatography. Journal of Chromatography A 1996. **740**: p. 1–9.
44. Inagaki, S.O., S.; Goto, Y.; Fukushima, Y., Mesoporous materials derived from layered silicates and the adsorption properties. Studies in Surface Science and Catalysis, 1998. **117**: p. 65–76.
45. Cesteros, Y.H., G. L. , Several factors affecting Al-MCM-41 synthesis. Microporous and Mesoporous Materials 2001. **43**: p. 171–179.
46. Coluccia, S.M., L.; Martra, G. , Characterisation of microporous and mesoporous materials by the adsorption of molecular probes: FTIR and UV–Vis studies. Microporous and Mesoporous Materials, 1999. **30**: p. 43–56.
47. Góra-Marek, K.D., IR studies of OH groups in mesoporous aluminosilicates. Applied Catalysis A: General, 2006. **302**(1): p. 104–109.
48. Hattori, H., Heterogeneous Basic Catalysis. Chemical Reviews, 1995. **95**: p. 537–558.
49. Hunger, M.S., U.; Breuninger, M.; Gläser, R.; Weitkamp,, Characterization of the acid sites in MCM-41-type materials by spectroscopic and catalytic techniques. J. Microporous and Mesoporous Materials 1999. **27**: p. 261–271.
50. Jentys, A.K., K.; Vinek, H. , Concentration of surface hydroxyl groups on MCM-41. Microporous and Mesoporous Materials, 1999. **27**: p. 321–328.
51. Ryoo, R.K., C. H.; Howe, R. F., Imaging the Distribution of Framework Aluminum in Mesoporous Molecular Sieve MCM-41. Chemistry of Materials 1997. **9**: p. 1607–1613.
52. Xu, M.W., W.; Seiler, M.; Buchholz, A.; Hunger, M. , Improved Brønsted Acidity of Mesoporous [Al]MCM-41 Material Treated with Ammonium Fluoride. The Journal of Physical Chemistry B, 2002. **106**: p. 3202–3208.
53. Lebeau, B.P., J.; Soulard, M.; Fowler, C.; Zana, R.; Vix-Guterl, C.; Patarin, Organized mesoporous solids: mechanism of formation and use as host materials to prepare carbon and oxide replicas. J. Comptes Rendus Chimie, 2005. **8**: p. 597–607.
54. Lee, J.H., S.; Hyeon, T., Synthesis of new nanoporous carbon materials using nanostructured silica materials as templates. Journal of Materials Chemistry, 2004. **14**: p. 478-486.
55. Lee, J.K., J.; Hyeon, T., Recent Progress in the Synthesis of Porous Carbon Materials. Advanced Materials, 2006. **18**: p. 2073–2094.
56. Lu, A.-H.S., F. , Nanocasting pathways to create ordered mesoporous solids. Comptes Rendus Chimie, 2005. **8**: p. 609–620.
57. Ryoo, R.J., S. H.; Jun, S., Synthesis of Highly Ordered Carbon Molecular Sieves via Template-Mediated Structural Transformation. The Journal of Physical Chemistry B, 1999. **103**: p. 7743–7746.
58. Ryoo, R.J., S. H.; Kruk, M.; Jaroniec, M., Ordered mesoporous carbons. Advanced Materials 2001. **13**: p. 677 - 681.

59. Y.-X. Jiang, Z.-F.C., Q.-C. Zhuang, J.-M. Xu, Q.-F. Dong, L. Huang, S.-G. Sun, A novel composite microporous polymer electrolyte prepared with molecule sieves for Li-ion batteries. Journal of Power Sources, 2006. **160**: p. 1320-1328.
60. J. Prochazka, L.K., M. Zukalova, O. Frank, M. Kalbac, A. Zukal, M. Klementova, D. Carbone, M. Graetzel, Novel Synthesis of the TiO2(B) Multilayer Templated Films. Chemistry of Materials, 2009. **21**: p. 1457- 1464.
61. J. Xi, X.Q., X. Ma, M. Cui, J. Yang, X. Tang, W. Zhu, L. Chen, Composite polymer electrolyte doped with mesoporous silica SBA-15 for lithium polymer battery. Solid State Ionics, 2005. **176**: p. 1249-1260.
62. L. Chen, B.Y., Y. Cao, K. Fan, Synthesis of Well-Ordered Mesoporous Titania with Tunable Phase Content and High Photoactivity. The Journal of Physical Chemistry C, 2007. **111**: p. 11849-11853.
63. H. Ding, H.S., Y. Shan, Preparation and characterization of mesoporous SBA-15 supported dye-sensitized TiO2 photocatalyst. Journal of Photochemistry and Photobiology A, 2005. **169**: p. 101-107.
64. F. Xia, E.O., L. Wang, J. Wang, Photocatalytic degradation of dyes over cobalt doped mesoporous SBA-15 under sunlight. Dyes and Pigments, 2008. **76**: p. 76-81.
65. H. Lachheb, O.A., A. Houas, J.P. Nogier, Photocatalytic activity of TiO2–SBA-15 under UV and visible light. Journal of Photochemistry and Photobiology A, 2011. **226**: p. 1-8.
66. C. Yang, Y.R.Z., Improved the performance of dye-sensitized solar cells by incorporating mesoporous silica (SBA-15) materials in scattering layer. J. Power Sources, 2012. **201**: p. 387-394.
67. Laura C. Kennedy, L.R.B., Nastassja A. Lewinski,Andrew J. Coughlin,Ying Hu,Emily S. Day, Jennifer L. West,Rebekah A. Drezek, A New Era for Cancer Treatment: Gold-Nanoparticle-Mediated Thermal Therapies. small, 2010. **7**: p. 169–183.
68. Hakami, O.Z., Y.; Banks, C., Thiol-functionalised mesoporous silica-coated magnetite nanoparticles for high efficiency removal and recovery of Hg from water. J. Water Research, 2012. **46**: p. 3913–3922.
69. Ke-Ni Yang, C.-Q.Z., Wei Wang, Paul C. Wang, Jian-Ping Zhou, and Xing-Jie Liang, pH-responsive mesoporous silica nanoparticles employed in controlled drug delivery systems for cancer treatment. Cancer Biol Med., 2014. **11**(1): p. 34–43.
70. Tang L, C.J., Nonporous silica nanoparticlesfor nanomedicine apllication Nano today, 2013. **8**: p. 290-312.
71. Horcajada, P.M.-A., C.; Rámila, A.; Pérez-Pariente, J.; Vallet-Regí, M. , Controlled release of Ibuprofen from dealuminated faujasites. Solid State Sciences, 2006. **8**: p. 1459–1465.
72. Andersson, J.R., J.; Areva, S.; Lindén, M. , Influences of Material Characteristics on Ibuprofen Drug Loading and Release Profiles from Ordered Micro- and Mesoporous Silica Matrices. Chemistry of Materials, 2004. **16**: p. 4160–4167.
73. Gao, Q.X., Y.; Wu, D.; Shen, W.; Deng, F., Synthesis, Characterization, and in Vitro pH-Controllable Drug Release from Mesoporous Silica Spheres with Switchable Gates. Langmuir 2010. **26**: p. 17133–17138.
74. Yu-fang Zhu, J.-l.S., , Yong-sheng Li, Hang-rong Chen, Wei-hua Shen, Xiao-ping Dong, Storage and release of ibuprofen drug molecules in hollow mesoporous silica spheres with modified pore surface. Microporous and Mesoporous Materials, 2005. **85**: p. 75–81.

75. Brian G. Trewyn, S.G., Igor I. Slowinga, Victor S.-Y. Lin, Mesoporous silica nanoparticle based controlled release, drug delivery, and biosensor systems. Chemical Communications, 2007: p. 3236-3245.
76. Trewyn, B.G.S., I. I.; Giri, S.; Chen, H.-T.; Lin, V. S. Y., Synthesis and Functionalization of a Mesoporous Silica Nanoparticle Based on the Sol–Gel Process and Applications in Controlled Release. Accounts of Chemical Research, 2007. **40**: p. 846–853.
. R. W. Kelsall, I.W.H., M. Geoghega, Nanoscale Science and Technology 2005.
78. Rotello, V.M., Nanoparticles: Building Blocks for Nanotechnology. springer, 2004.
79. Miltat, A.T.a.J., Small Is Beautiful. Science, 1999: p. 1939.
80. Goldman, A., Modern Ferrite Technology Van Nostrand Reinhold, New York,, 1990.
81. Murthy, B.V.a.V.R.K., Ferrite Materials: Science and Technology. Narosa Publishing House, New Delhi, 1990.
82. Wijn, J.S.a.H.P.J., Ferrites Philips Technical Library, 1959.
83. Baldi, G.B., D.; Innocenti, C.; Lorenzi, G.; Sangregorio, C, Cobalt ferrite nanoparticles: The control of the particle size and surface state and their effects on magnetic properties. J. Magn. Magn. Mater, 2007. **311**: p. 10-16.
84. Rudolf Hergt, S.D., Magnetic particle hyperthermia—biophysical limitations of a visionary tumour therapy. J. Magn. Magn. Mater., 2007. **311**: p. 187–192.
85. Stéphane Mornet, S.V., Fabien Grasseta ,Etienne Duguet, Magnetic nanoparticle design for medical diagnosis and therapy. Journal of Materials Chemistry, 2004. **14**: p. 2161-2175.
86. S. L oucrent, D.F., M. Port, A. Roch, C. Robic, L. Vander Elst, R. N. Muller, Magnetic Iron Oxide Nanoparticles: Synthesis, Stabilization, Vectorization, Physicochemical Characterizations, and Biological Applications. Chem. Rev, 2008. **108**.
87. T. Kikumori, T.K., M. Sawaki, T. I mai,, Anti-cancer effect of hyperthermia on breast cancer by magnetite nanoparticle-loaded anti-HER2 immunoliposomes. Breast Cancer Research and Treatment, 2009. **113**.
88. Jaime Santoyo Salazar, L.P., Oscar de Abril, Lai Truong Phuoc, Dris Ihiawakrim, Manuel Vazquez, Jean-Marc Greneche, Sylvie Begin-Colin, and Genevieve Pourroy, Magnetic Iron Oxide Nanoparticles in 10−40 nm Range: Composition in Terms of Magnetite/Maghemite Ratio and Effect on the Magnetic Properties. Chem. Mater, 2011. **23**(6): p. 1379–1386.
89. Joshi, H.M., Lin Yen, P., Aslam, M., Prasad, P.V., Schultz-Sikma, E.A., Edelman, R., Meade, T., Dravid, V.P., Effects of Shape and Size of Cobalt Ferrite Nanostructures on Their MRI Contrast and Thermal Activation. J. Phys. Chem. C, 2009. **113**: p. 17761–17767.
90. Z. T. Chen, L.G., Synthesis and magnetic properties of CoFe2O4 nanoparticles by using PEG as surfactant additive. Materials Science and Engineering: B, 2007. **141**(1-2): p. 82–86.
91. Z. H . L i, T.P.Z., X. Y. Zhan, D. S. Gao, Q. Z. Xiao, G. T. Li, High capacity three-dimensional ordered macroporous CoFe2O4 as anode material for lithium ion batteries. Electrochim. Acta, 2010. **55**(15): p. 4594–4598.
92. Y. Wang, D.S., A. Ung, J.-ho A hn, G. Wang, Hollow CoFe2O4 nanospheres as a high capacity anode material for lithium ion batteries. Nanotechnology, 2012. **23**.
93. Arruebo, M., Fernández-Pacheco, R., Ibarra, M.R., Santamaría, Magnetic nanoparticles for drug delivery. J. Nanotoday, 2007. **22**(3): p. 22–32.

94. Chemla, Y.R., Grossman, H.L., Poon, Y., McDermott, R., Stevensi, R., Alper, M.D., Clarke, J., Proc., Ultrasensitive magnetic biosensor for homogeneous immunoassay. Natl. Acad. Sci. U.S.A, 2000. **97**(26): p. 14268–14272.
95. Hergt, R., Dutz, S., Muller, R., Zeisberger, M., Magnetic particle hyperthermia: nanoparticle magnetism and materials development for cancer therapy. Journal of Physics: Condensed Matter, 2006. **18**.
96. Salloum, M., Ma, R.H., Weeks, D., Zhu, L., Controlling nanoparticle delivery in magnetic nanoparticle hyperthermia for cancer treatment: Experimental study in agarose gel. Int. J. Hyperthermia 2008. **24**(4).
97. Hansu Birol, C.R.R., Marcela Guiotokuc, Dachamir Hotza, Preparation of ceramic nanoparticles via cellulose-assisted glycine nitrateprocess: a review. RSC Adv., 2013. **3**: p. 2873-2884.
98. C Lam, Y.F.Z., Y.H Tang, C.S Lee, I Bello, S.T Lee, Large-scale synthesis of ultrafine Si nanoparticles by ball milling. Journal of Crystal Growth, 2000. **220**(4): p. 466–470.
99. Gao, G., Nanostructures and nanomaterials: synthesis, properties and applications. London: Imperial College Press, 2004.
100. Mahmoud Goodarz Naseri, E.B.S., Hossein Abbastabar Ahangar, Abdul Halim Shaari and Mansor Hashim, Simple Synthesis and Characterization of Cobalt Ferrite Nanoparticles by a Thermal Treatment Method. Journal of Nanomaterials, 2010. **2010**: p. 8.
101. M. H. Khedr, A.A.O., and S. A. Abdel-Moaty, Magnetic nanocomposites: preparation and characterization of Coferrite nanoparticles. Colloids and Surfaces A: Physicochemical and Engineering Aspects, 2006. **281**(1-3): p. 8-14.
102. Z. Zi, Y.S., X. Zhu, Z. Yang, J. Dai, and W. Song, Synthesis and magnetic properties of CoFe2O4 ferrite nanoparticles. Journal of Magnetism and Magnetic Materials, 2009. **321**(9): p. 1251–1255.
103. J. B. Silva, W.D.B., and N. D. S. Mohallem, Influence of heat treatment on cobalt ferrite ceramic powders. Materials Science and Engineering B, 2004. **112**(2-3): p. 182–187.
104. Rinaldi, V.L.C.-D.a.C., Synthesis and magnetic characterization of cobalt-substituted ferrite (CoxFe3−xO4) nanoparticles. Journal of Magnetism and Magnetic Materials, 2007. **314**(1): p. 60–67.
105. D. Zhao, X.W., H. Guan, and E. Han, Study on supercritical hydrothermal synthesis of CoFe2O4 nanoparticles. Journal of Supercritical Fluids, 2007. **42**(2): p. 226–233.
106. L. Chen, Y.S., and J. Bai, Large-scale synthesis of uniform spinel ferrite nanoparticles from hydrothermal decomposition of trinuclear heterometallic oxo-centered acetate clusters. Materials Letters, 2009. **63**(12): p. 1099–1101.
107. Gharagozlou, M., Synthesis, characterization and influence of calcination temperature on magnetic properties of nanocrystalline spinel Co-ferrite prepared by polymeric precursor method. Journal of Alloys and Compounds, 2009. **486**(1-2): p. 660–665.
108. Maqsood, H.G.a.A., Structural, magnetic and electrical properties of cobalt ferrites prepared by the sol-gel route,. Journal of Alloys and Compounds, 2008. **465**(1-2): p. 227– 231.
109. Shah, V.P.a.D.O., Synthesis of high-coercivity cobalt ferrite particles using water-in-oil microemulsions,. Journal of Magnetism and Magnetic Materials, 1996. **163**: p. 243– 248.
110. Lan, J.Z.a.C.Q., Laser-generated Ni and Co nanoparticles in organic media. Materials Letters, 2008. **62**(10-11): p. 1521–1524.

REFERENCES

111. G. Baldi, D.B., C. Innocenti, G. Lorenzi, and C. Sangregorio, Cobalt ferrite nanoparticles: the control of the particle size and surface state and their effects on magnetic properties. Journal of Magnetism and Magnetic Materials, 2007. **311**(1): p. 10–16.
112. K. V. P. M. Shafi, A.G., R. Prozorov, and J. Balogh, Sonochemical preparation and size-dependent properties of nanostructured CoFe2O4 particles Chemistry of Materials. **10**(11): p. 3445–3450.
113. S. Singhal, J.S., S. K. Barthwal, and K. Chandra, Preparation and characterization of nanosize nickel-substituted cobalt ferrites (Co1−xNixFe2O4),. Journal of Solid State Chemistry, 2005. **178**(10): p. 3183–3189.
114. S. Choi, M.-H.C., A review on the relationship between aloe vera components and their biologic effects. Seminars in Integrative Medicine, 2003. **1**(1): p. 53-62.
115. T. Reynolds, A.C.D., Aloe vera leaf gel: a review update. Journal of Ethnopharmacology, 1999. **68**(1-3): p. 3–37.
116. K.H. Shin, W.S.W., S.S. Lim, C.S. Shim, H.S. Chung, E.J. Kennely, A.D. Kinghorn, Elgonica-Dimers A and B, Two Potent Alcohol Metabolism Inhibitory Constituents of Aloe arborescens. J. Nat. Prod, 1997. **60**(11): p. 1180–1182.
117. K. Umano, K.N., A. Shoji, T. Shibamoto Elgonica-Dimers A and B, Two Potent Alcohol Metabolism Inhibitory Constituents of Aloe arborescens. J. Agric. Food Chem, 1999. **47**: p. 3702.
118. D. Saccu, P.B., G.J. Procida, Aloe Exudate: Characterization by Reversed Phase HPLC and Headspace GC-MS. J. Agric. Food Chem, 2001. **49**.
119. A. Lodha, M.L., A. Patel, J. Chaudhuri, J. Dalal, M. Edwards, and D. Douroumis, Synthesis of mesoporous silica nanoparticles and drug loading of poorly water soluble drug cyclosporin A. J Pharm Bioallied Sci, 2012.
120. Limin Guo, Y.F.a.N.T., Vapor phase synthesis of mesoporous silica rods within the pores ofalumina membranes. New J. Chem, 2012. **36**: p. 1301-1303.
121. Hao Xu, F.Y., Eric E. Monson and Raoul Kopelman, Room-temperature preparation and characterization of poly (ethylene glycol)-coated silica nanoparticles for biomedical applications. Journal of Biomedical Materials Research Part A, 2003. **66A**(4): p. 870-879.
122. Tan, S.S.K.W.R.T.W., Development of novel dye-doped silica nanoparticles for biomarker application. Journal of Biomedical Optics, 2001. **1**: p. 160-166.
123. Anna Bonamartini Corradi, F.B., Anna Maria Ferrari, Bonaventura Focher, Cristina Leonelli, Synthesis of silica nanoparticles in a continuous-flow microwave reactor. Powder Technology, 2006. **167**(1): p. 45–48.
124. Kim S. Finnie , J.R.B., Christophe J. A. Barbé and Linggen Kong, Formation of Silica Nanoparticles in Microemulsions. Langmuir, 2007. **23**(6): p. 3017–3024.
125. Van Hai Le , C.N.H.T.a.H.H.T., Synthesis of silica nanoparticles from Vietnamese rice husk by sol–gel method Nanoscale Research Letters, 2013.
126. Kota Sreenivasa Rao, K.E.-H., Tsutomu Kodaki, Kazumi Matsushigea, Keisuke Makino, A novel method for synthesis of silica nanoparticles. Journal of Colloid and Interface Science, 2005. **298**(1): p. 125–131.
127. Huichen Guo, H.Q., Shiqi Sun, Dehui Sun, Hong Yin, Xuepeng Cai, Zaixin Liu, Jinyan Wu ,Tao Jiang, Xiangtao Liu Hollow mesoporous silica nanoparticles for intracellular delivery of fluorescent dye. Chemistry Central Journal, 2011.
128. bindhani B.K., p.A.K., Green Synthesis of Gold Nanoparticles using Neem leaf extract and its Biomedical Applications. 2014. **5**: p. 457-464.

129. Prashant Mohanpuria, N.K.R., Sudesh Kumar Yadav, Biosynthesis of nanoparticles: technological concepts and future applications. Journal of Nanoparticle Research, 2008. **10**(3): p. 507-517.
130. Jenny P. Glusker, M.L., Miriam Ross, Crystal Structure Analysis for Chemists and Biologists. Vch publishers, 1994.
131. Singh, R.J., solid state physics. Dorling Kndersley, 2012.
132. Ebsworth, E.A.V.R., David W. H. Cradock, Stephen., Structural methods in inorganic chemistry. 1987.
133. Zhen Guo, L.T., Fundamentals and Applications of Nanomaterials. Artech House, 2009.
134. West, A.R., solid state chemistry and its applications. Wiley Vch Verlag Company, 1984.
135. Cullity, B.D., introduction to magnetic materials. Addison Wesley Publishing Company, 1972.
136. S Amenlinckx, D.v.D., J van Landuyt, Handbook of Microscopy, Applications in Material Science. Solid State Physics and Chemistry Methods I,VCH Weinheim, 1997.
137. G.Venkataraman, Quantum revolution: Qed: the jewel of physics. universities press, 1994. **2**.
138. Gerhard Dehm, J.M.H., Josef Zwec, In-situ Electron Microscopy: Applications in Physics, Chemistry and material science. Wiley Vch Verlag Compant 2012.
139. Fu-Yun Zhu, Q.-Q.W., Xiao-Sheng Zhang, Wei Hu, Xin Zhao and Hai-Xia Zhang, 3D nanostructure reconstruction based on the SEM imaging principle, and applications. Nanotechnology, 2014. **25**(18).
140. Pillai, S.O., Solid State Physics ,revised sixth edition. New age international publishers, 2005. **6**.
141. Swann, G.E.A.a.P., S. V., Application of Fourier Transform Infrared Spectroscopy (FTIR) for assessing biogenic silica sample purity in geochemical analyses and palaeoenvironmental research. Climate of the Past, 2011. **7**(1): p. 65-74.
142. Zanyar Movasaghi, S.R.D.I.u.R., Fourier Transform Infrared (FTIR) Spectroscopy of Biological Tissues. Applied Spectroscopy Reviews, 2008. **43**(2).
143. Thomas, M.J.K.A., David J., Ultraviolet and visible spectroscopy. AGRIS, 1996.
144. Wang, J., Multiwalled Boron Nitride Nanotubes: Growth, Properties, and Applications. p. 23-44.
145. B.J. Clark, T.F., M.A. Russell, UV Spectroscopy: Techniques, instrumentation and data handling. 1993: p. 6-23.
146. David Greene , R.S.-G., Joseph Govan and Yurii K. Gun'ko, Synthesis Characterization and Photocatalytic Studies of Cobalt Ferrite-Silica-Titania Nanocomposites. Nanomaterials, 2014. **4**(2): p. 331-343.
147. Chitra, K.a.A., G., Fluorescent silica nanoparticles in the detection and control of the growth of pathogen. Journal of Nanotechnology, 2013.
148. Stanley, R. and A.S. Nesaraj, Effect of Surfactants on the Wet Chemical Synthesis of Silica Nanoparticles. International Journal of Applied Science and Engineering 12 (1), 2014: p. 9-21.
149. Piaoping Yang, Z.Q., Lanlan Lu, Shanshan Huang, Jun Li,, Luminescence functionalization of mesoporous silica with different morphologies and applications as drug delivery systems. Biomaterials, 2008. **29**(6): p. 692–702.
150. Zhang, G., Xu, Y., Xu, D., Wang, D., Xue, Y., Su, W., Pressure-induced crystallization of amorphous SiO2 with silicon-hydroxy group and the quick synthesis of coesite under lower temperature. High Pressure Res, 2008. **28**.
151. Bao Chena, G.Q., Zhouhua Wang, Jianwen Chen, Linna Wu, Yuehong Xu, Ge Li, Chuanbin Wu, Hollow mesoporous silicas as a drug solution delivery system for insoluble drugs. Powder Technology, 2013. **240**: p. 48–53.

152. A. Sousa, K.C.S., E.M.B. Sousa, Mesoporous silica/apatite nanocomposite: Special synthesis route to control local drug delivery. Acta Biomaterialia, 2008. **4**(3): p. 671–679.
153. Hu, J.B., Y.; Zhan, J.; Yuan, X.; Sekiguchi, T.; Golberg, D., Self-assembly of SiO2 nanowires and Si microwires into hierarchical heterostructures on a large scale. Adv. Mater, 2005. **17**: p. 971–975.
154. Chitra, K. and G. Annadurai, Fluorescent silica nanoparticles in the detection and control of the growth of pathogen. Journal of Nanotechnology, 2013. **2013**.
155. Yan-Tao Shi, H.-Y.C., Yi Geng, Hai-Ming Nan, Wei Chen, Qiang Cai, Bao-Hua Chen, Xiao-Dan Sun, You-Wei Yao, Heng-De Li, The size-controllable synthesis of nanometer-sized mesoporous silica in extremely dilute surfactant solution. Materials Chemistry and Physics, 2010. **120**(1): p. 193–198.